**CENTRO DE INVESTIGACIÓN Y DE ESTUDIOS AVANZADOS**
**DEL INSTITUTO POLITÉCNICO NACIONAL**

Unidad Mérida

**DEPARTAMENTO DE FÍSICA APLICADA**

# "Exploración sistemática de las Superficies de Energía Potencial de las estequiometrías $C_6H_{6-n}Li_n$ (n = 1 – 6) y $C_6E_6$ (E = Li – Cs)"

TESIS

Que presenta

**Jorge Javier Pedrozo Romero**

Para obtener el grado de

**Maestro en Ciencias**

en

**Fisicoquímica**

Director de Tesis:

**Dr. José Gabriel Merino Hernández**

Mérida, Yucatán, México

Septiembre de 2020

CENTRO DE INVESTIGACIÓN Y DE ESTUDIOS AVANZADOS
DEL INSTITUTO POLITÉCNICO NACIONAL

Unidad Mérida

DEPARTAMENTO DE FÍSICA APLICADA

# “A Systematic Exploration of the Potential Energy Surface of $C_6H_{6-n}Li_n$ (n = 1 – 6) and $C_6E_6$ (E = Li - Cs) stoichiometries”

a tesis submitted by:

**Jorge Javier Pedrozo Romero**

In partial fulfillment of the requirements for the degree of

**Master of Sciences**

in

**Physical Chemistry**

Thesis Advisor:

**Dr. José Gabriel Merino Hernández**

Mérida, Yucatán, México September of 2020

# AGRADECIMIENTOS

Quiero agradecer profundamente a mis amigos de la maestría por embarcarse en esta odisea en aguas desconocidas. A Francisco por tenderme una mano cuando lo necesité, por ser mi cómplice en los antojos y mi aprendiz de química. A José Luis por soltar siempre su veneno (con buena intención, hay que aclarar), hacerme reflexionar sobre muchos temas y ser una persona en quien confiar. A *Gera* por las charlas inolvidables, el conocimiento y los *hacks* que compartió conmigo. A *George* por sus excelentes sugerencias que elevaron la calidad de este trabajo. Por falta de espacio, pero no por importancia, quiero agradecer a todo el personal del CINVESTAV, a los investigadores que nos impartieron clases y la Dra. Veleva por su valiosa amistad.

Al Dr. Merino, quién me brindó la gran oportunidad de trabajar con su excelente equipo de trabajo. A mis sinodales, el Dr. Ortíz y el Dr. Ruíz, por sus oportunas correcciones y comentarios.

Por último, mi eterna gratitud y cariño a mi mamá Edith y a mi abuela, quienes han velado por mí, apoyándome para que sea una mejor persona y profesionista.

“I have attempted to give you a glimpse... of what there may be of soul in chemistry. But it may have been in vain. Perchance the chemist is already damned and the guardian of the pearly gates had decreed that of all the black arts, chemistry is the blackest. But if the chemist has lost his soul, he will not have lost his courage and as he descends into the inferno, sees the rows of glowing furnaces and sniffs the homey fumes of brimstone, he will call out -*Asmodeus, hand me a test tube*.”

*Gilbert Newton Lewis*

## Resumen

Los compuestos organolitiados suelen presentar geometrías y estructuras completamente diferentes con respecto a sus análogos en los hidrocarburos. Ejemplo de ello es la supuesta síntesis del hexalitiobenceno, que en un principio se asumió que la estructura era similar a la del benceno, pero tras posteriores revisiones y estudios teóricos, se llegó a la conclusión que la estructura bencenoide de la estequiometría $C_6Li_6$ es de muy alta energía y hallándose un cúmulo asimétrico de tres fragmentos $C_2Li_2$ como el mínimo global para este sistema molecular. Dados el comportamiento del litio para favorecer estructuras *no clásicas*; así como diversas aplicaciones en síntesis, catálisis y en la elaboración de las baterías recargables, es nuestro interés explorar las superficies de energía potencial (PES por sus siglas en inglés) de los sistemas estequiométricos $C_6H_{6-n}Li_n$ ($n = 1 - 6$) y $C_6E_6$ (E = Li – Cs). Las exploraciones se llevaron a cabo de forma sistemática y exhaustiva empleando GLOMOS (Global Optimization of Molecular Systems) con un barrido inicial a PBE0/def2-SVP para localizar las estructuras más estables para cada sistema. Dichas estructuras fueron reoptimizadas a TPSS+D3(BJ)/def2-TZVP incluyendo las correcciones de la energía en el punto cero (ZPE por sus siglas en inglés). La discusión energética de las tres estructuras más estables en cada sistema se realizó a CCSD(T)/def2-TZVP//TPSS+D3(BJ)/def2-TZVP, mientras que los enlaces fueron estudiados bajo el esquema de Orbitales Naturales de Enlace (NBO por sus siglas en inglés) y con la metodología de la Partición Adaptativa de la Densidad Natural (AdNDP por sus siglas en inglés). Los resultados muestran que la baja sustitución de los hidrógenos del benceno por litio ($n = 1$ o $2$) no afectan la estructura del anillo, por otro lado, los litios transfieren de manera efectiva su carga a los carbonos del benceno y contribuyen a la estabilización de la carga para formar aniones $C_6H_5^-$ y $C_6H_4^{2-}$. Al aumentar el grado de sustitución ($n = 3 - 6$) la ruptura del enlace C-C es promovida por la inserción de los átomos de litio en el anillo, lo que promueve la apertura del sistema anillado y la formación de fragmentos organolitiados más pequeños que tienden a parecerse a $C_2Li_2$. Los sistemas $C_6Li_6$ y $C_6Na_6$ prácticamente muestran las mismas estructuras estables, diferenciándose solo en el tamaño de enlace C-E (E = Li, Na). En cambio, los sistemas $C_6E_6$ de los metales alcalinos más pesados (K, Rb y Cs) presentan un comportamiento totalmente distinto, en donde las estructuras más estables presentan iones alcaluros ($E^-$) y enlaces E-E (E = K, Rb y Cs). El tamaño relativo de los iones de litio y sodio permiten que exista contacto directo con los átomos de carbono y por lo tanto la transferencia de carga es efectiva. En contraste, no todos los átomos de los metales alcalinos son capaces de establecer contacto directo con los átomos de carbono, en cambio transfieren parte de su carga a los átomos metálicos vecinos,

promoviendo la estabilización de los enlaces E-E (K, Rb y Cs) y la formación de los iones $E^-$.

# Abstract

The organolithium compounds usually have different structures and geometries with respect their hydrocarbons analogues. An example of this is the supposed synthesis of hexalithiobenzene, compound whose structure was assumed to be like benzene, but after several revisions and theoretical studies it was concluded that the benzenoid structure with $C_6Li_6$ stoichiometry is very high in energy, and an asymmetrical cluster of three $C_2Li_2$ units was found as the global minimum for this molecular system. Given the tendency of lithium to favour *non classical* structures, as well its applications in organic synthesis, catalysis and its importance in rechargeable batteries; it is our interest to explore the Potential Energy Surfaces (PES) of $C_6H_{6-n}Li_n$ (n = 1 – 6) and $C_6E_6$ (E = Li – Cs) stoichiometries. The systematic and exhaustive explorations were carried out with GLOMOS (Global Optimization of Molecular Systems) with an initial screening at PBE0/def2-SVP level, to locate the most stable structures. Then such structures were refined at TPSS+D3(BJ)/def2-TZVP level of theory, including the Zero-Point Energy corrections (ZPE). The energetic discussion of the three lowest-lying energy structures for each system was at CCSD(T)/def2-TZVP//TPSS+D3(BJ)/def2-TZVP level, meanwhile the bonding pattern was studied in terms of Natural Bonding Orbitals (NBO), and with the Adaptative Natural Density Partitioning (AdNDP) methodology. Our results show that a lower rate of hydrogen substitution by lithium atoms (n = 1 or 2 ) in benzene molecule does not affect the structure of the ring, the lithium atoms transfer all its charge to the skeletal carbons and contribute to the stabilization of $C_6H_5^-$ and $C_6H_4^{2-}$ anions. Increasing the rate of substitution (n = 3 – 6) the cleavage of C-C bonds is favoured by the insertion of lithium atoms, which promotes the breaking of the ring and the formation of smaller organic fragments that leads to $C_2Li_2$ units. The lithium and sodium stoichiometries ($C_6Li_6$ and $C_6Na_6$) present the same lowest-lying energy structures, where only the C-E distance is different (E = LI or Na). Instead the heavier alkali metal stoichiometries $C_6E_6$ (E = K, Rb and Cs) present different lowest-lying energy structures, which alkalides ions ($E^-$) and E-E bonds are stabilized. The relatively small size of the lithium and sodium ions allow a direct contact with the skeletal carbon atoms, hence an effective charge transfer. On the other hand, not all the heavier alkaline metal atoms are able a direct contact with the carbon atoms, instead they transfer part of its charge to vicinal metal atoms, therefore promoting the formation of alkalide ions ($E^-$) and the stabilization of E-E bonds.

# Index

# List of figures

# List of schemes and tables

# General introduction

Organolithium structures do not follow classical rules: the replacement of a hydrogen by lithium atom in an organic molecule almost always leads to a major change in geometry, electronic state, or both.[1] For instance, several computations indicate that dilithiomethane $CH_2Li_2$ contains a planar tetracoordinate carbon rather than tetrahedral, with similar energies for both singlet and triplet; or dilithioethylene is predicted to have double bridged structure rather than a planar one (**Figure 1-a**).[2,3] West showed that perlithiated propyne in butyllithium excess gives one of the most stable lithiocarbons, $C_3Li_4$. Although there is still no detailed experimental information available, his computations indicate a remarkable structure with a W-shaped Li-CCC-Li backbone and two symmetrical bridging lithiums (**Figure 1-b**).[4] Another exciting study case is $C_5Li_4$, a compound obtained by West and Klein experimentally by perlithiation of penta-1,3-diyne. There are a high number of possible ways in which four lithium atoms can be arranged around a C atom. After examined all possible arrangements (cages, clusters, planar structures, etc.), they found that the most stable structure is compromised by $C_2Li_2$ and $C_3Li_4$ units sharing two lithium atoms in common (**Figure 1-d**), followed 37 kcal/mol above by Li-CCCCC-Li system with a five-coordinated central lithium ion (**Figure 1-c**).[4]

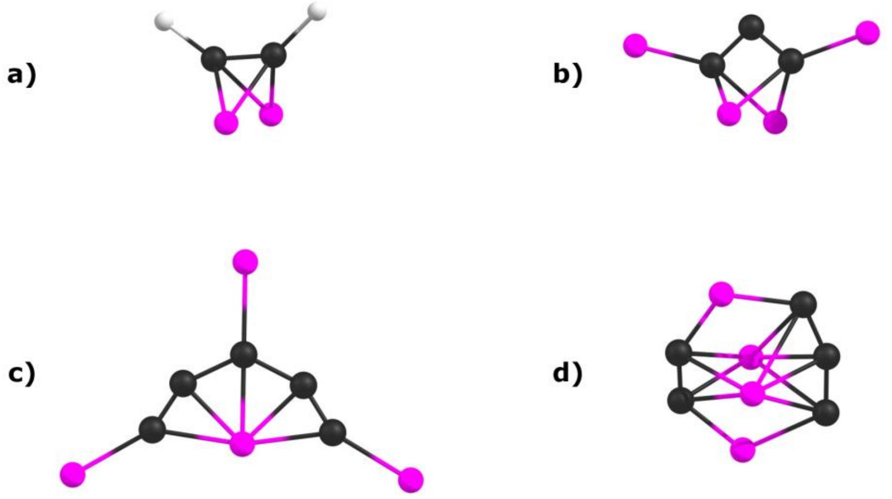

***Figure 1**. Some bonding representations in organolithium compounds: a) vicinal bonding, b) 1,3-arrangement, c) multiple bonding, and d) two organic fragments arrangement.*

The formation of such nonclassical structures is induced, in part, for the type of bond between carbon and lithium. The electronegativity difference between C and Li strongly suggests that the C-E bond (E = Li - Cs) is ionic. However, the solubility of some organolithium compounds in nonpolar solvents, such as benzene, indicates a covalent character.[5] Efforts have been made to model and understand the nature of the C-E bond, both experimental and theoretical approaches. One of the simplest models to study the C-E bond is using methyl derivatives. In 1996, Bickelhaupt and coworkers investigated the monomers, dimers, and tetramers of $CH_3Li$ using Density Functional Theory (DFT) and conventional ab initio Molecular Orbital Theory.[6] This study highlighted the role of a covalent component in the C-Li bond, especially in the $CH_3Li$ tetramer, explaining the experimental large coupling constants observed in NMR spectroscopy.[7] However, some studies advocate the ionic character of the C-Li bond. Kwon et al. reported the Natural Population Analysis (NPA), charges, and dipole moments of $CH_3Li$, *t*-BuLi, and PhLi oligomers, indicating an ionic character of the organolithium bond in such systems.[8]

One of the most representative cases is hexalithiobenzene, which was allegedly synthesized by Lagow in 1990. In their report, they proposed a benzene-type structure for the compound although scarce or no evidence was provided. It was until 2013, after several revisions and theoretical studies that a structure more stable than the assumed benzene-type was proposed.

Given the tendency of lithium and the rest of the alkali metals to favor non classical structures, it is our interest to identify the most stable structures of some representative organoalkalimetal compounds. This work focuses on the systematic exploration of the potential energy surface (PES) of the $C_6H_{6-n}Li_n$ (n = 1 - 6) and $C_6E_6$ (E = Na – Cs) systems. We decided on these systems as a milestone towards future research on lithium batteries.

The thesis is organized as follows: In **Chapter 1** (Theoretical background) - the computational details are specified. In **Chapter 2** (lithium stoichiometries) - our computations show that if the rate of lithium substitution in benzene is low (1 or 2), the ring shape is maintained. In all the $C_6H_{6-n}Li_n$ systems, the lithium atoms transfer their charge almost entirely to the carbon atoms, so increasing the rate of substitution (3 to 6) induces the ring breaking and the charge from lithium atoms is distributed among several smaller organic fragments and hydride ions. In **Chapter 3** (hexaalkali stoichiometries) - two tendencies were identified. The first one is that the lighter alkali metals (Li and Na) share similar arrangements. The second one is that the heavier alkali metals (K, Rb and Cs) tend to partially transfer their charge to the carbon atoms, thus favoring alkalide-type structures and triplets as global minima. **Chapter 4** (Conclusions) - chemical and structural similarities of the studied systems are further discussed; conclusions and future perspectives to include $C_6H_{6-x}E_x$ (E = Na to Cs, x = 1 - 6) in future works are given.

# Chapter 1. Theoretical background

## *Potential Energy Surface (PES)*

The Potential Energy Surface (PES) is an abstract concept in chemistry. This mathematical function relates the energy of a molecular system to the different spatial arrangements of its atoms. Consider a polyatomic molecule made up of *n* atoms, whose spatial coordinates are $q_n = (x_n, y_n, z_n)$ and assume that the molecule behaves like balls (atoms) held together by springs (chemical bonds), we can define a function $E = f(q_1, q_2, q_3, \dots, q_n)$, which depicts a *n-dimensional* surface of the potential energy of the molecule, that is, the Potential Energy Surface (PES). Thus, every possible arrangement is associated with a point on the surface.$^{9}$

Among them, the stationary points are of particular interest in chemistry. Mathematically, a stationary point is one when the first derivative of the potential energy with respect each spatial coordinate is zero:

$$\frac{\partial E}{\partial q_1} = \frac{\partial E}{\partial q_2} = \frac{\partial E}{\partial q_3} = \cdots = \frac{\partial E}{\partial q_n} = 0$$

Stationary points where the second derivative is positive, independently of the direction, are known as a *minima*. Whereas those points where the second derivative is negative on the path that connects two minima are known as saddle points.

Once a stationary point has been found, a calculation of the vibrational frequencies is done to determine if that point corresponds to a minimum or a saddle point. Such calculation requires: a) the use of the second derivatives of the energy with the spatial coordinate *q* as force constants, and b) the PES have to be quadratically curved along each geometric coordinate, which is only true in the vicinity of a stationary point. A minimum on the PES has all the normal-mode force constants positive: for each vibrational mode there is a restoring force, like that of a spring. But for a transition state, just one of the vibrations, corresponding along the path that connects two minima is different. Since the force constants are related to the second derivatives of the energy and they are negative only on the reaction path, the force constant for this mode is negative. So, a transition state (a first-order saddle point) has one and only one negative normal-mode force constant, and since the frequency calculation involves taking the square root of a force constant, that gives an imaginary number.

Thus, a transition state has one imaginary frequency corresponding to the reaction coordinate.[10]

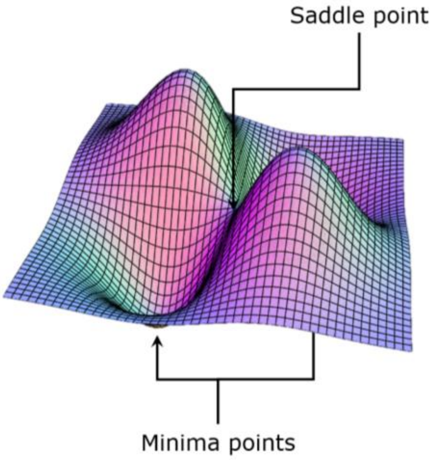

***Figure 2**. Qualitative 3D representation of a potential energy surface, where the saddle and minima points are indicated.*

In this work, we explored the PES in order to locate and characterize the most stable structures, lowest-lying minima, for the $C_6H_{6-n}Li_n$ (n = 1 - 6) and $C_6E_6$ (E = Li - Cs) molecular clusters using a heuristic search algorithm (GLOMOS).[11]

### *GLOMOS – Global Optimization of Molecular Systems*

In computer science, a heuristic (from Greek εὑρίσκω "I find" or "discover") is a technique designed for solving a problem more quickly when classical methods are too slow, or for finding an approximate solution when conventional methods fail to find an exact solution.

Among them, Genetic Algorithms (GA) achieved enough popularity as a method of optimization and machine learning.[12] The GAs are search algorithms based on Darwinian natural selection and mimic the genetic mechanisms present in organisms. GLOMOS is a suite of heuristic search algorithms, written in python, that includes a set of methodologies to find the putative global minimum in molecular systems, where the DFT local optimizations are solved using electronic structure codes such as *Gaussian 16*.[13]

The adopted procedure in GLOMOS is as follows: the algorithm generates the first batch of families of structures (according to preestablished geometrical patterns), which are optimized at a low level of theory, then an energy fitness parameter is defined in terms of the potential energy and dictates how well adapted is each individual of each family. Next, the algorithm selects the most adapted structures of each family, and a simple one-point crossover accomplishes the exchange of genetic information. This part of the procedure distinguishes the GAs from other stochastic strategies. The new structures (children) will give birth to new families, some random mutations are introduced, and the algorithm repeats itself until the optimal structure (lowest potential energy) is achieved (**Figure 3**).[14]

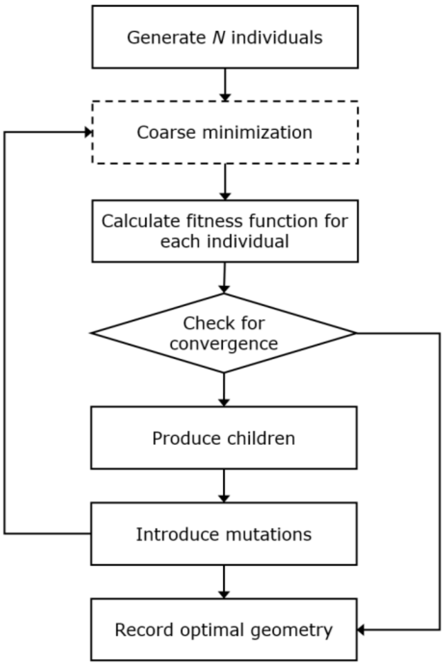

***Figure 3**. Flow chart of a standard genetic algorithm.*

### *Computational details*

The PESs of the $C_6H_{6-n}Li_n$ (n = 1 - 6) clusters were explored systematically using a genetic algorithm (GA) implemented in the GLOMOS program. As already explained in the previous section, it is our interest to locate the stationary points associated particularly, the putative global minima, Thus, the search was not limited to ring structures, but includes linear, branched and cluster arrangements.

First, the case in which a single lithium substitutes a hydrogen atom in the $C_6H_6$ stoichiometry was examined. Subsequently, systems derived from the progressive increase of the number of lithium atoms, as well as

$C_6E_6$ (E = Na - Cs) were considered. An initial screening search was performed at the PBE0/def2-SVP level, this hybrid functional includes a quarter of the exact HF exchange energy with three quarters of the PBE GGA exchange energy. This functional was chosen because it reproduces with enough accuracy molecular structures and properties of the majority of the elements of the periodic table.[15] On the other hand, the def2-SVP basis set, developed by Ahlrichs and coworkers, contains polarizing and diffuse functions for a wide range of *p* and *d* elements. This basis set has successfully been used to obtain qualitatively correct results.[16]

The structures obtained by the exploration and whose relative energies did not exceed 40 kcal/mol with respect the putative global minimum were further re-optimized at the TPSS+D3(BJ)/def2-TZVP level, including the Grimme's D3 dispersion approach. The functional TPSS is a GGA method which generally gives excellent results for a wide range of systems and has a good performance at predicting bond lengths in organic molecules, hydrogen-bonded complexes and ionic solids.[17] Although PBE0 also gives comparable results to TPSS, the latter has a practical advantage since it is not a hybrid functional and does not depend on parametrizations. The def2-TZVP is a larger set used mainly for optimization purposes, since the errors in computed bond lengths typically are smaller than one pm and that in bond angles smaller than one degree for most DFT methods.

One disadvantage of DFT methods is its inability to describe long-range correlations sufficiently. However, such interactions are indispensable to obtain interaction energies with errors less than the common chemical accuracy of 1 kcal/mol, particularly for non-covalently bond systems. Therefore, semiclassical dispersion corrections to DFT have been developed in the past years and are meanwhile used routinely in many quantum chemistry codes. Some of these correction schemes accurately incorporate London dispersion into DFT at very small computational costs. A variety of different dispersion correction schemes has been proposed. In this work, we considered the dispersion forces through the Grimme D3 approximation with the Becke-Johnson (BJ) damping function.[18]

Single point energies of the lowest structures were estimated at the CCSD(T)/def2-TZVP//TPSS+D3(BJ)/def2-TZVP level. The CCSD(T) method is now well-established as a highly accurate and cost-effective technique for the calculation of the structures and properties of atoms and molecules. It is mainly used to predict with high accuracy structural data and chemical properties. So, the discussion of energies will correspond to those obtained at this level.[19] For each structure, a frequency analysis was done and none of them has any imaginary frequency.

The chemical bonding was studied by Natural Bond Orbital (NBO) scheme and the Adaptive Natural Density Partitioning (AdNDP) methodology. The NBO is a sequence of natural localized orbital sets that include natural atomic, hybrid and semi-localized molecular orbital (NLMO) sets, that is intermediate between basis atomic orbitals and canonical molecular orbitals (MOs). Such NBOs provide the most accurate possible *natural Lewis structure* picture of the structure because all orbital details (polarization coefficients, atomic hybrid compositions, etc.) are mathematically chosen to include the highest possible percentage of the electron density.[20] On the other hand, the AdNDP is a method of description of the chemical bonding with an intuitive simplicity of Lewis theory and generality of canonical orbital theory. It is based on the concept of the electron pair as the main element of chemical bonding, thus it represents the electronic structure in terms of $nc$ - $2e^-$ bonds, where n is the total number of atoms where the bond is taking place. One feature of the AdNDP analysis is that it recovers Lewis bonding and delocalized bonding elements.[21] Finally, all the computations were made using the Gaussian 16 version.[13]

# Chapter 2. Lithium stoichiometries

### *$C_6H_5Li$ stoichiometry*

Our computations at the CCSD(T)/def2-TZVP//TPSS+D3(BJ)/def2-TZVP level show that the global minimum for such stoichiometry is **A-01**, phenyllithium (**Figure 4**), which is basically the direct lithium substitution of one hydrogen atom in benzene. It adopts $C_{2v}$ symmetry, where all C-C (1.395 - 1.416 Å) and C-H bonds (1.088 - 1.093 Å) are quite similar to those in benzene (1.390 Å and 1.090 Å, respectively). The WBI value of 0.184 for the C-Li bond indicates a predominantly ionic character, which is also supported by the computed NPA charges at Li and C (+0.89 and -0.62 $|e^-|$, respectively). So, the structure could be visualized as the interaction between the $C_6H_5^-$ carbanion with a $Li^+$ cation. The calculated C-Li bond (1.965 Å) is in excellent agreement with the reported 1.970 Å for the monomer at B3LYP/6-31+G* level.[8]

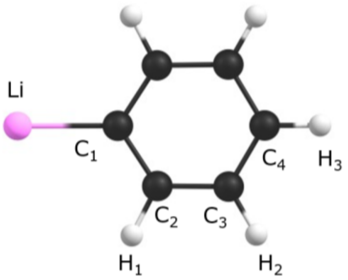

**A-01**

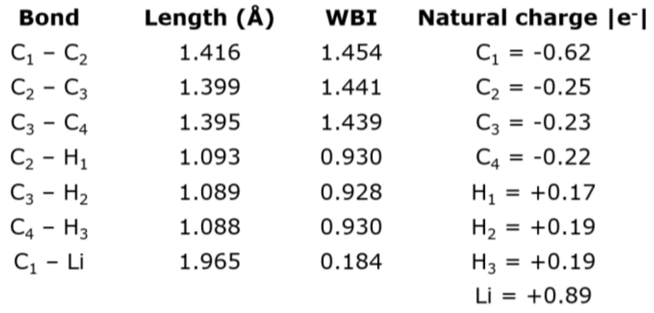

| Bond | Length (Å) | WBI | Natural charge $|e^-|$ |
|---|---|---|---|
| $C_1 - C_2$ | 1.416 | 1.454 | $C_1$ = -0.62 |
| $C_2 - C_3$ | 1.399 | 1.441 | $C_2$ = -0.25 |
| $C_3 - C_4$ | 1.395 | 1.439 | $C_3$ = -0.23 |
| $C_2 - H_1$ | 1.093 | 0.930 | $C_4$ = -0.22 |
| $C_3 - H_2$ | 1.089 | 0.928 | $H_1$ = +0.17 |
| $C_4 - H_3$ | 1.088 | 0.930 | $H_2$ = +0.19 |
| $C_1$ – Li | 1.965 | 0.184 | $H_3$ = +0.19 |
| | | | Li = +0.89 |

***Figure 4**. Bond lengths are given in Å, Wiberg bond index and NPA charges in $|e^-|$.*

Phenyllithium is known to be a tetramer in diethyl ether, but a dimer without any Lewis-base ligand. In 1998, Dinnebier et al. resolved the structure of the phenyllithium in the solid state and it is also a tetramer (**Figure 5**).[22] Two kinds of C-Li interactions can be distinguished, one is the $C_{aryl}$ – Li σ-bond of 2.242 Å and the second is the $C_{phenyl}$ – Li π bonds of 2.401 - 2.862 Å. Note that both C-Li distances are longer than those computed in the gas phase.

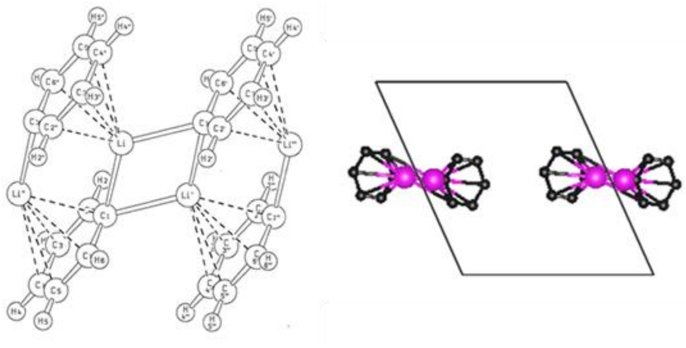

***Figure 5**. Crystal structure of the solid-state phenyllithium. In the image on the right, the hydrogen atoms were removed to improve the appreciation of the structure. The pink spheres represent lithium atoms and the black ones carbon atoms.*[22]

Our AdNDP analysis in **A-01** (**Figure 6**)shows an electron pair with an occupation number (ON) of 1.82 |e$^-$|, localized at C1, 6 C-C σ-bonds (ON = 1.98 | e$^-$|), 5 C-H σ-bonds (ON = 1.98 | e$^-$|), and 3 π-bonds (ON = 1.94 | e$^-$|). The recovered Lewis structure is aromatic since it meets the Hückel rule (6 π-electrons).[23] Thus we can assume that the lithium practically transfers all its charge directly to the carbon skeleton, without inducing any significant geometrical change in the ring.

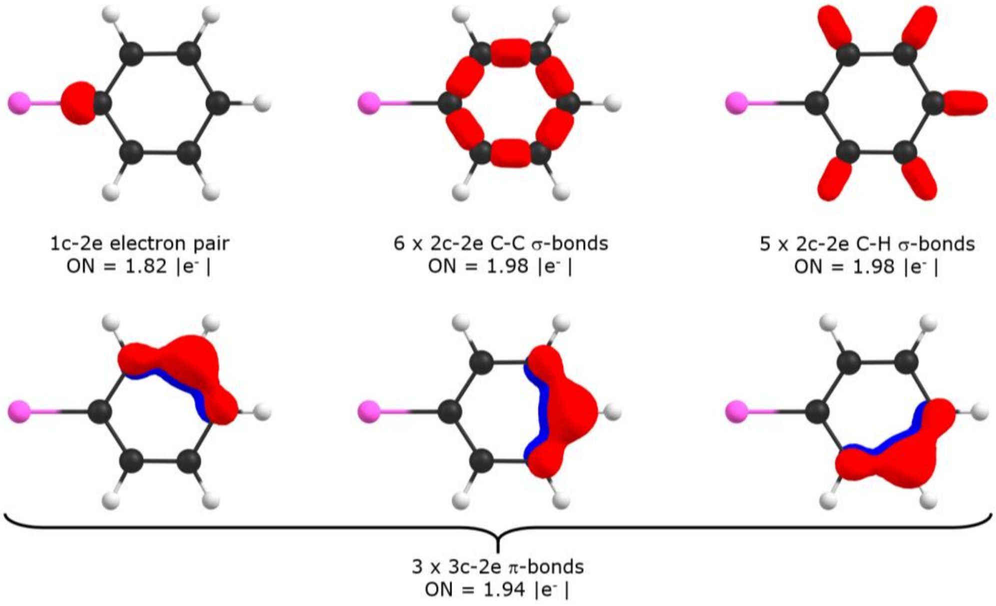

***Figure 6**. AdNDP analysis for **A-01** (ON is the occupation number).*

The second lowest-lying energy form is **A-02**. The energy difference between **A-02** and the global minimum is 11.4 kcal/mol (CCSD(T)/def2-TZVP//TPSS+D3(BJ)/def2-TZVP). In this arrangement the six-membered ring is preserved (**Figure 7**). The lithium atom is located above the ring with C-Li bonds with lengths of 2.165 to 2.261 Å, which are closer to the experimental value in the crystal of 2.242 Å for the $C_{aryl}$ – Li σ bond in $(PhLi)_4$.[22] The WBI for the C-Li bonds are less than 0.100 threshold, which also indicates that the C-Li interaction is essentially ionic. The charge of the lithium is slightly higher (+0.92 $|e^-|$) than in **A-01**, indicating that the location above the ring improves the charge transfer from the lithium to the carbon atoms. Meanwhile charges of the carbons are in -0.29 to -0.37 $|e^-|$, suggesting that the lithium atom behaves as a cation interacting with the $\pi$-cloud of the carboanion skeleton.

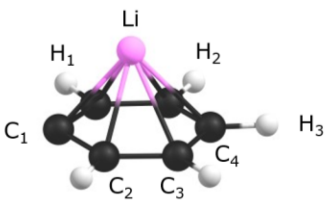

**A-02**

| Bond | Length (Å) | WBI | Natural charge $|e^-|$ |
|---|---|---|---|
| $C_1 - C_2$ | 1.429 | 1.437 | $C_1$ = -0.37 |
| $C_2 - C_3$ | 1.411 | 1.432 | $C_2$ = -0.34 |
| $C_3 - C_4$ | 1.406 | 1.406 | $C_3$ = -0.29 |
| $C_1$ – Li | 2.139 | 0.073 | $C_4$ = -0.31 |
| $C_2$ – Li | 2.135 | 0.016 | $H_1$ = +0.19 |
| $C_3$ – Li | 2.231 | 0.019 | $H_2$ = +0.21 |
| $C_4$ – Li | 2.261 | 0.017 | $H_3$ = +0.21 |
| C – H | 1.090 | 0.920 | Li = +0.92 |

***Figure 7**. Bond lengths are given in Å, Wiberg bond index and NPA charges in $|e^-|$.*

The exhaustive exploration was carried out up to 40 kcal/mol, where the stable structures (**Figure 8**) can be organized as follows: (a) up to 10 kcal/mol above from the global minimum, only benzene-type arrangements were found (**A-01** and **A-02**), (b) between 10 and 30 kcal/mol fulvene-type structures ($C_5H_4CH^-$) were located (**A-03** and **A-04**) (c) between 30 and 40 kcal/mol, linear and branched geometries (**A-05**, **A-07** and **A-08**, respectively) compete with fulvene-type structures (**A-06**), and the first triplet is located at 41.2 kcal/mol (**A-09**).

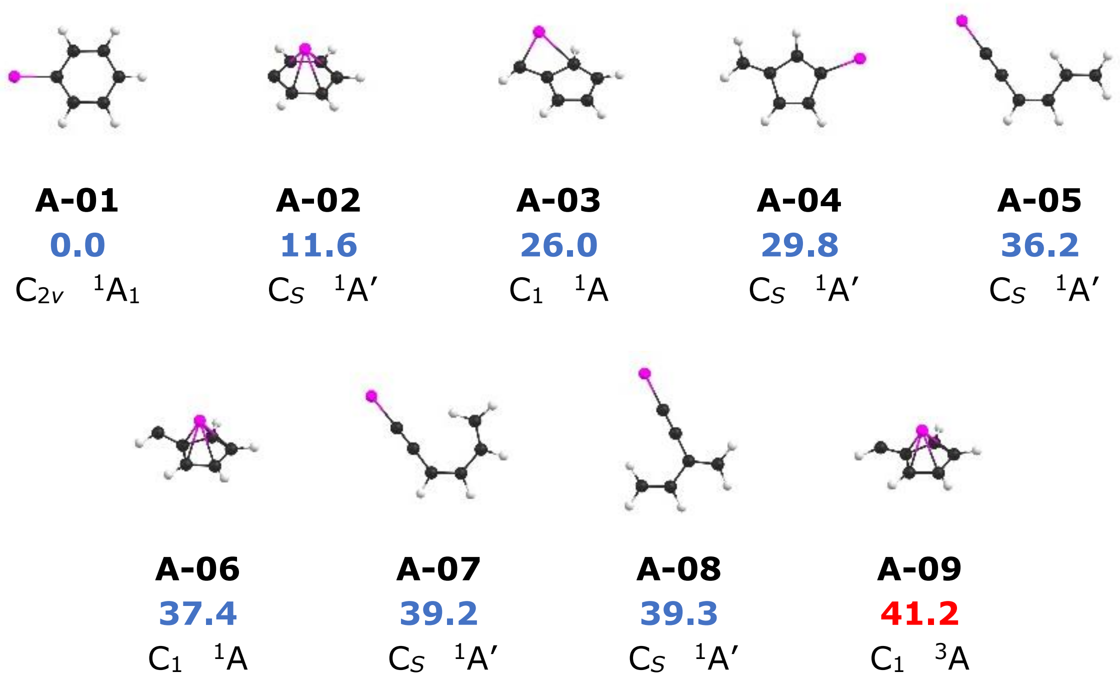

***Figure 8**. Lower-lying energy structures up to 40 kcal/mol above the global minimum for $C_6H_5Li$ stoichiometry. The relative energies are given by the **bolded blue (singlets)** and **red values (triplets)** in kcal/mol. Relative energies are at the TPSS+D3(BJ)/def2-TZVP level including the zero-point energy (ZPE) corrections.*

### ***$C_6H_4Li_2$ stoichiometry***

The putative global minimum **B-01** adopts a $C_s$ symmetry with one of the lithiums bridging two carbon atoms with the shorter C-Li bonds (1.913 Å). The Li above the ring is coordinated with the entire ring (**Figure 9**), showing larger C-Li bond lengths (2.124 - 2.210 Å). The computed charges are +0.93 $|e^-|$ for the lithium above the ring, and +0.88 $|e^-|$ for the lithium bonded to both carbon atoms with -0.67 $|e^-|$. The low WBI values (less than 0.100) corroborate that the larger C-Li bonds have more ionic character than the shorter ones (0.103).

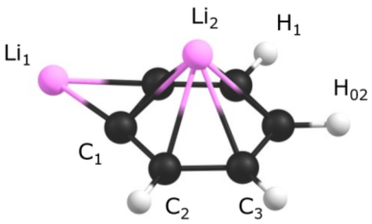

**B-01**

| Bond | Length (Å) | WBI | Natural charge $|e^-|$ |
|---|---|---|---|
| $C_1 - C_1$ | 1.468 | 1.478 | $C_1$ = -0.67 |
| $C_1 - C_2$ | 1.417 | 1.452 | $C_2$ = -0.32 |
| $C_2 - C_3$ | 1.412 | 1.420 | $C_3$ = -0.31 |
| $C_3 - C_3$ | 1.407 | 1.429 | H = +0.19 |
| $C_1 - Li_1$ | 1.913 | 0.103 | $Li_1$ = +0.88 |
| $C_1 - Li_2$ | 2.124 | 0.037 | $Li_2$ = +0.93 |
| $C_2 - Li_2$ | 2.158 | 0.017 | |
| $C_3 - Li_2$ | 2.210 | 0.018 | |
| C – H | 1.089 | 0.910 | |

***Figure 9**. Bond lengths are given in Å, Wiberg bond index and NPA charges in |e-|.*

The AdNDP analysis for **B-01** shows two electron pair localised on both C2 (ON = 1.84 |e-|), 6 C-C σ-bonds (ON = 1.98 |e-|), 4 C-H σ-bonds (ON = 1.98 |e-|) and 3 π-bonds (ON = 1.94 |e-|). Therefore, both lithiums virtually transfer all their charge to the carbon ring and the structure can be understood as C6H42- carbanion with two Li+ stabilizing the charge (**Figure 10**).

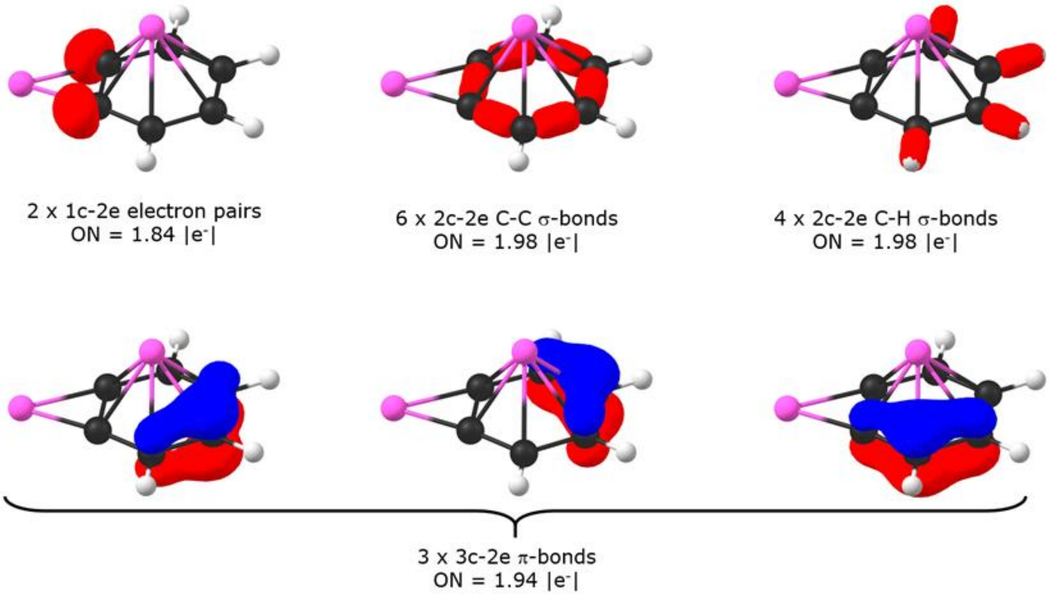

2 x 1c-2e electron pairs
ON = 1.84 $|e^-|$

6 x 2c-2e C-C $\sigma$-bonds
ON = 1.98 $|e^-|$

4 x 2c-2e C-H $\sigma$-bonds
ON = 1.98 $|e^-|$

3 x 3c-2e $\pi$-bonds
ON = 1.94 $|e^-|$

***Figure 10**. AdNDP analysis for **B-01** (ON is the occupation number).*

**B-02** has $C_{2v}$ symmetry and is located 4.45 kcal/mol (CCSD(T)/def2-TZVP//TPSS+D3(BJ)/def2-TZVP) above the global minimum. Both lithiums are bonded out of the plane to both C1 atoms while interacting with each other. The C-Li bonds are 1.978 Å with a WBI value of 0.114, indicating that they have an important ionic character (**Figure 11**). The charge of both lithium atoms is slightly lower (+0.86 $|e^-|$) than those in **B-01**, suggesting that such geometry affects the charge transfer from the lithiums to the carbon atoms. Also, our computations show that the organolithium carbon charge is -0.77 $|e^-|$ meanwhile the carbons are -0.24 and -0.23 $|e^-|$. Unlike the previous structure, the charge transfer from the lithiums to the carbon atoms seems affected due to the position of the second $Li^+$ since it cannot interact with the $\pi$-cloud of the carbon ring.

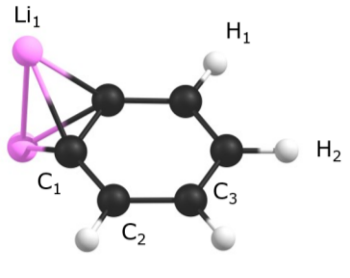

**B-02**

| Bond | Length (Å) | WBI | Natural charge \|e⁻\| |
|---|---|---|---|
| $C_1 - C_1$ | 1.455 | 1.531 | $C_1$ = -0.77 |
| $C_1 - C_2$ | 1.407 | 1.436 | $C_2$ = -0.24 |
| $C_2 - C_3$ | 1.399 | 1.444 | $C_3$ = -0.23 |
| $C_3 - C_3$ | 1.399 | 1.435 | H = +0.19 |
| $C_1 - Li_1$ | 1.978 | 0.114 | $Li_1$ = +0.86 |
| $Li_1 - Li_1$ | 2.557 | 0.011 | |
| C – H | 1.091 | 0.918 | |

***Figure 11**. Bond lengths are given in Å, Wiberg bond index and NPA charges in |e⁻|.*

The next isomer **B-03** is located 8.1 kcal/mol above the global minimum and adopts $C_s$ symmetry where all atoms lie on the plane (**Figure 12**). The lithium bonded to both carbons have different lengths (1.877 and 1.974 Å) but similar WBI (0.112 and 0.121) indicating that all the C-Li have a predominant ionic character. The charges for both lithiums are quite similar (+0.82 and +0.86 |e⁻| respectively) but for the carbons change drastically according to the proximity with the lithium atoms. At C5, C4 and C6 are -0.76, -0.34 and -0.57 |e⁻| respectively; and for the remaining three carbons are -0.22 and -0.23 |e⁻|.

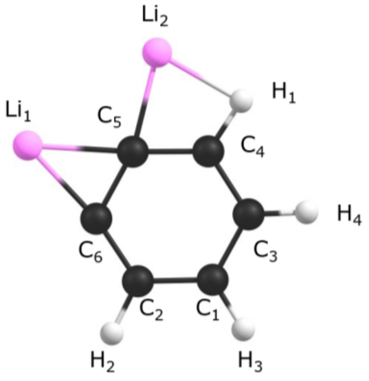

**B-03**

| Bond | Length (Å) | WBI | Natural charge \|e⁻\| |
|---|---|---|---|
| $C_5 - C_4$ | 1.415 | 1.451 | $C_1$ = -0.22 |
| $C_4 - C_3$ | 1.397 | 1.417 | $C_2$ = -0.22 |
| $C_3 - C_1$ | 1.395 | 1.441 | $C_3$ = -0.23 |
| $C_1 - C_2$ | 1.400 | 1.437 | $C_4$ = -0.34 |
| $C_2 - C_6$ | 1.404 | 1.444 | $C_5$ = -0.76 |
| $C_6 - C_5$ | 1.425 | 1.468 | $C_6$ = -0.57 |
| $C_6 - Li_1$ | 1.877 | 0.112 | $H_1$ = +0.10 |
| $C_5 - Li_1$ | 1.974 | 0.121 | H = +0.19 |
| $C_5 - Li_2$ | 1.905 | 0.185 | $Li_1$ = +0.82 |
| $H_1 - Li_2$ | 1.815 | 0.011 | $Li_2$ = +0.86 |

***Figure 12**. Bond lengths are given in Å, Wiberg bond index and NPA charges in |e⁻|.*

Although synthesis of dilithiobenzene has been reported since the end of the 1950's,[24] and its isomers (*ortho*-, *meta*-, and *para*-

dilithiobenzene),[25,26] the assumption of the formation of these species was based on the results of derivatization with several electrophiles.[27–29] Theoretical studies about the electronic structure of dilithiobenzene are scarce in the literature, and a few DFT studies only considered a few forms containing six-membered rings. In such study, Bachrach and Miller examine the structures of all the possible polylithiated benzenes compounds using computational techniques.[30,31] For dilithiobenzene they examined *ortho*-, *meta*-, and *para*- substitution positions (**Figure 13**) as well as locations where the lithium atoms can bridge two or six carbons atoms. They reported a structure, which corresponds to **B-02**, as the global minimum for dilithiobenzene. These classical structures (such as presented **in Figure 13**) were located within our exhaustive exploration: *para*- (**B-07**, 13.9 kcal/mol), *meta*- (**B-11**, 14.7 kcal/mol) and *ortho*-dilithiobenzene (**B-19**, 21.2 kcal/mol). These results show that neither of these structures correspond to the global minimum for dilithiobenzene, since lithium atoms prefer to bridge several carbon atoms or interact with the $\pi$-cloud of the ring system, hence the importance to carry out extensive explorations.

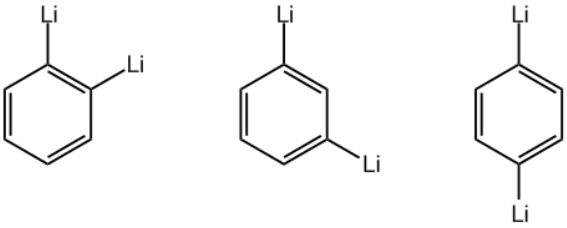

***Figure 13**. Isomers of dilithiobenzene.*

The assumption of the formation of these species was based on the results of derivatization with several electrophiles. Still, such conclusions may be erroneous since the electrophiles and lithiating reagent (generally *tert*-butyllithium) may co-exist to some extent with the dilithiated species and hence the formation of a di-functionalized product may be the result of a double consecutive lithium exchange reaction (**Scheme 1**).[32]

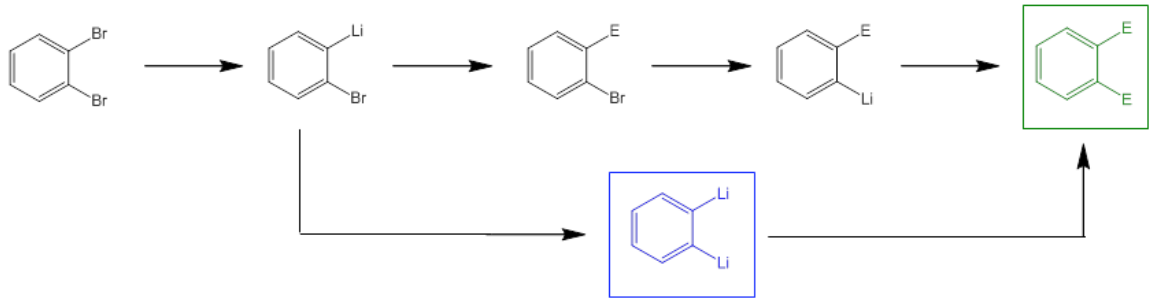

***Scheme 1**. Mechanism for the halogen-metal exchange of 1,2-dibromobenzene, where a dilithiobenzene intermediary (blue) is possible.*[32]

Some patterns can be appreciated among the lower-lying energy structures up to 40 kcal/mol above the global minimum. (a) within the 20 kcal/mol, the 75% of the geometries are benzene-type structures (**Figure 14**), (b) between 20 and 40 kcal/mol most of the structures are linear or branched geometries (about 75%) and the few benzene-shaped ones are triplets (more results and structures are located in the supplementary section of this work).

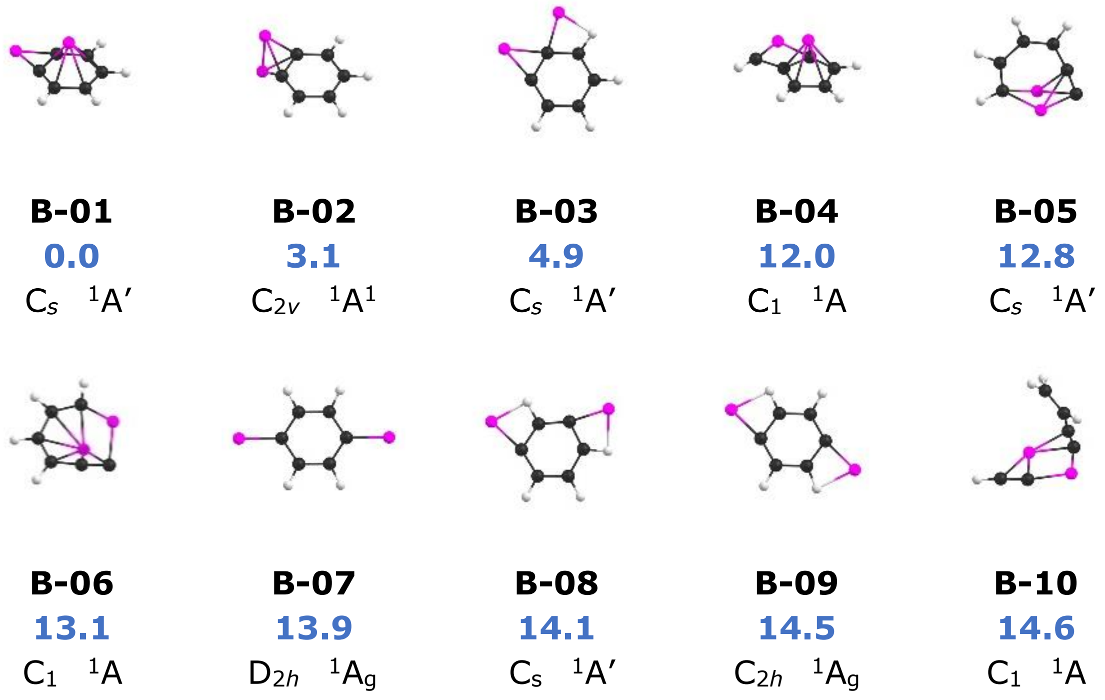

**B-01** **0.0** $C_s$ $^1A'$

**B-02** **3.1** $C_{2v}$ $^1A^1$

**B-03** **4.9** $C_s$ $^1A'$

**B-04** **12.0** $C_1$ $^1A$

**B-05** **12.8** $C_s$ $^1A'$

**B-06** **13.1** $C_1$ $^1A$

**B-07** **13.9** $D_{2h}$ $^1A_g$

**B-08** **14.1** $C_s$ $^1A'$

**B-09** **14.5** $C_{2h}$ $^1A_g$

**B-10** **14.6** $C_1$ $^1A$

***Figure 14**. Ten lowest-lying energy structures for $C_6H_4Li_2$ stoichiometry. The relative energies are given by the bolded blue values (singlets) in kcal/mol. Relative energies are at the TPSS+D3(BJ)/def2-TZVP level of theory including the zero-point energy (ZPE) corrections.*

### $C_6H_3Li_3$ *stoichiometry*

The exploration for such a combination shows a hydride-type compound **C-01** as the global minimum. In this structure, the lithiums promote the cleavage of C-C and C-H bonds, then one of them locates at the center of the figure, making it quasi-planar, and the other two lithium atoms stabilize the hydride ion. This arrangement adopts a $C_s$ symmetry where the plane cuts the figure in half (**Figure 15**).

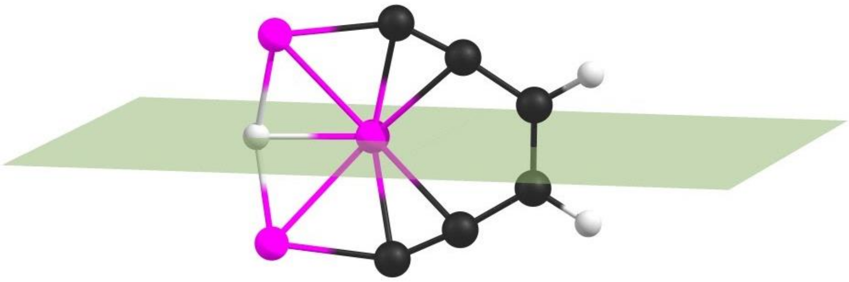

***Figure 15**. Zenith view of **C-01** with the symmetry plane that cuts in half the structure.*

This form has two triple C-C bonds (1.245 Å, WBI = 2.746), two single C-C bonds (1.416 Å, WBI = 1.178) and one double C-C bond (1.367 Å, WBI = 1.678). The Li-H bonds (1.784 and 1.931Å) are longer than the reported for lithium hydride (1.595 Å).[33,34] The central C-Li bonds are longer (2.101 and 2.250 Å) than the perimeter ones (1.989 Å), whose WBI are less than 0.100 and 0.111, respectively. Which indicates that the central C-Li bonds are again essentially ionic. The charge on the terminal carbons is -0.61 |e$^-$|, for the hydride is -0.82 |e$^-$| and for the central lithium is +0.82 |e$^-$| and +0.89 |e$^-$| for the perimeter ones, and +0.22 |e$^-$| at H2. (**Figure 16**)

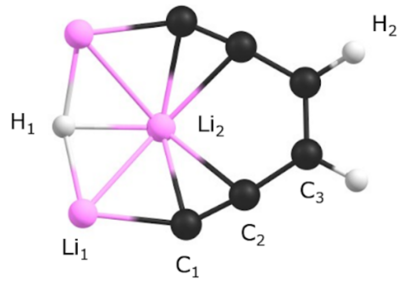

**C-01**

| Bond | Length (Å) | WBI | Natural charge \|e$^-$\| |
|---|---|---|---|
| $C_1 - C_2$ | 1.245 | 2.746 | $C_1$ = -0.61 |
| $C_2 - C_3$ | 1.418 | 1.178 | $C_2$ = -0.25 |
| $C_3 - C_3$ | 1.367 | 1.678 | $C_3$ = -0.24 |
| $C_1 - Li_1$ | 1.989 | 0.111 | $H_1$ = -0.82 |
| $C_1 - Li_2$ | 2.101 | 0.084 | $H_2$ = +0.22 |
| $C_2 - Li_2$ | 2.250 | 0.019 | $Li_1$ = +0.89 |
| $Li_2 - Li_2$ | 2.472 | 0.009 | $Li_2$ = +0.82 |
| $H_1 - Li_2$ | 1.784 | 0.086 | |
| $H_1 - Li_2$ | 1.931 | 0.099 | |
| $C_3 - H_2$ | 1.088 | 1.088 | |

***Figure 16**. Bond lengths (Å), Wiberg bond index and NPA charges |e$^-$| of **C-01** for $C_6H_3Li_3$ stoichiometry.*

The AdNDP analysis shows and electron pair localized in H1 (ON = 1.82 |e$^-$|), which corroborates its hydride character, two electron pairs on both C1 (ON = 1.87 |e$^-$|), five C-C σ-bonds (ON = 1.98 |e$^-$|), two C-H σ-bonds (ON = 1.97 |e$^-$|), three C-C $\pi$-bonds (ON = 1.88 |e$^-$|) and two C-C $\pi$-bonds (ON = 1.95 |e$^-$|). For this structure, the charge transfer from the lithiums induces the cleavage of one C-C bond in the benzene, followed by the insertion of the lithium cations to stabilize a hydride ion ($H^-$) and the organic fragment $C_6H_2^{2-}$ (**Figure 17**).

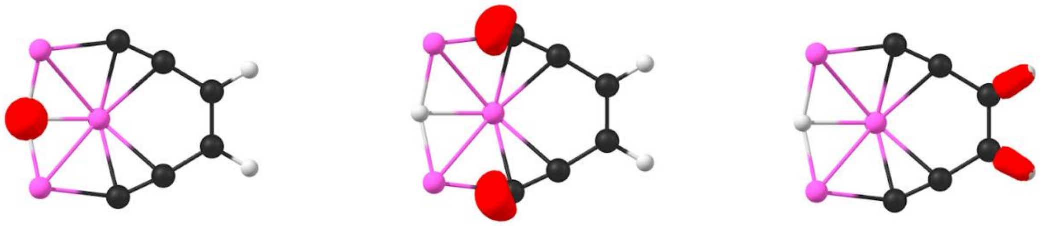

1c-2e electron pair
ON = 1.82 $|e^-|$

2 x 1c-2e electron pairs
ON = 1.87 $|e^-|$

2 x 2c-2e C-H σ-bonds
ON = 1.97 $|e^-|$

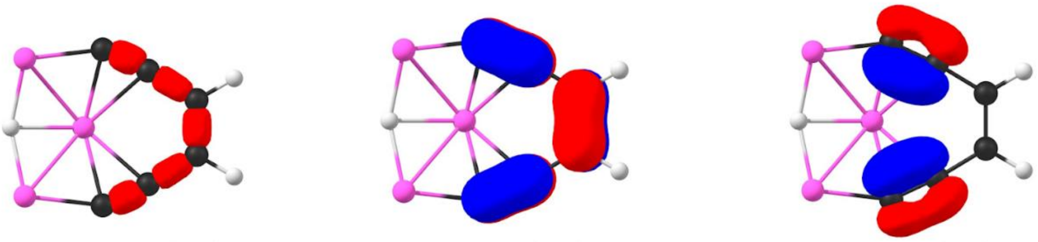

5 x 2c-2e C-C σ-bonds
ON = 1.98 $|e^-|$

3 x 2c-2e π-bonds
ON = 1.88 $|e^-|$

2 x 2c-2e π-bonds
ON = 1.95 $|e^-|$

***Figure 17**. AdNDP analysis for **C-01** (ON is the occupation number).*

Located at 4.9 kcal/mol (at CCSD(T)/def2-TZVP level) above the global minimum is **C-02**, a benzene-type arrangement with $C_s$ symmetry, where one of the lithiums is above the ring and a pentacoordinate carbon atom (C1). The C-C and C-H bonds (1.412 - 1.448 Å for C-C and 1.092 Å for C-H) are quite similar to those in benzene, the C-Li bonds above the ring are longer (2.097 - 2.187 Å) than those on the plane (1.893 and 1.962 Å). The WBI for the C-Li is less than 0.100 for the longer bonds. The computed NPA charges on Li1 and both Li2 are +0.83 and +0.93 $|e^-|$, respectively. In this structure, the overall charge transfer from the lithiums to the carbons is slightly higher than in C-01 (+2.59 and +2.53 $|e^-|$, respectively), although the energy required to maintain the benzene ring makes **C-02** the second lowest-energy structure (**Figure 18**).

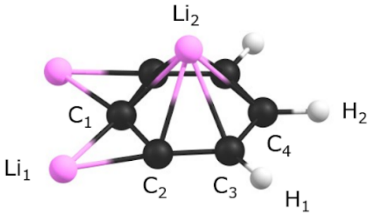

**C-02**

| Bond | Length (Å) | WBI | Natural charge $|e^-|$ |
|---|---|---|---|
| $C_1 - C_2$ | 1.448 | 1.473 | $C_1$ = -0.88 |
| $C_2 - C_3$ | 1.417 | 1.436 | $C_2$ = -0.66 |
| $C_3 - C_4$ | 1.412 | 1.426 | $C_3$ = -0.33 |
| $C_1 - Li_1$ | 1.962 | 0.143 | $C_4$ = -0.30 |
| $C_2 - Li_1$ | 1.893 | 0.112 | H = +0.20 |
| $C_1 - Li_2$ | 2.097 | 0.026 | $Li_1$ = +0.83 |
| $C_2 - Li_2$ | 2.153 | 0.029 | $Li_2$ = +0.93 |
| $C_3 - Li_2$ | 2.157 | 0.017 | |
| $C_4 - Li_2$ | 2.187 | 0.019 | |
| C – H | 1.092 | 0.920 | |

***Figure 18**. Bond lengths (Å), Wiberg bond index and NPA charges $|e^-|$ of **C-02** for $C_6H_3Li_3$ stoichiometry.*

Due to their high value as synthetic intermediaries, several attempts had been made to obtain highly polylithiated benzenes, but most have failed to count a few exceptions, such as the reports of the synthesis of 1,3,5-trilithiobenzene by halogen/metal exchange reaction in extreme conditions,[35] and the claimed synthesis of the hexalithiobenzene. In this regard, it is worth mentioning the work carried out by Schlosser and coworkers in which they made several attempts to obtain trilithiobenzene by the triple substitution of trifluorobenzene but were able to only interchange at most two.[35] For trilithiobenzene, Bachrach and Miller examined 1,2,3-; 1,3,5-; 1,2,4- substitution positions as well as one or two lithium bridging all the carbon atoms.[30,31] They claimed **C-02** as the global minimum for the $C_6H_3Li_3$ combination, and concluded that any attempt to substitute three or more halogens by lithium in halobenzene will fail. Thus, as the degree of substitution increases, disproportionation reactions begin to compete and therefore the exchange reaction becomes unfavorable.

In contrast, our results show that the charge transfer from the lithium atoms to carbon skeleton promotes the cleavage of C-C bonds by the insertion of one or all the lithium atoms into the ring. Most of them present linear or branched geometries, as well as arrangements of two organic fragments ($C_2H^-$ and $C_4H_2^{2-}$) or $H^-$ ions (**Figure 19**). Benzene shaped triplets were located at 35 kcal/mol or higher energies with respect to the global minimum (see supplementary section).

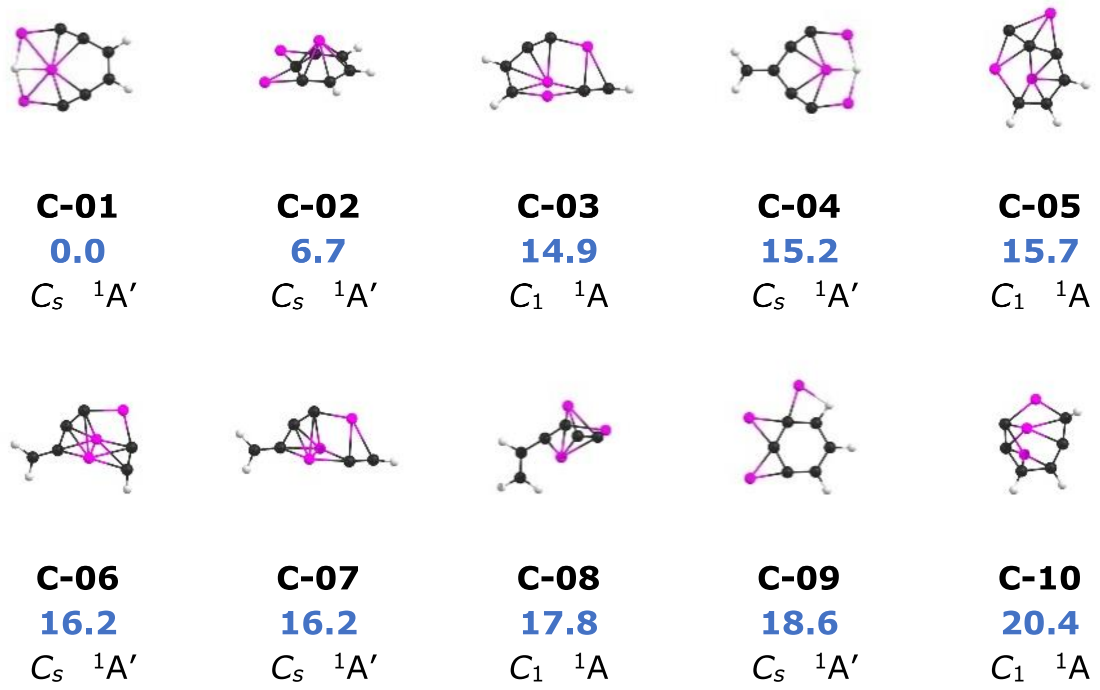

**C-01**
**0.0**
$C_s$ $^1$A′

**C-02**
**6.7**
$C_s$ $^1$A′

**C-03**
**14.9**
$C_1$ $^1$A

**C-04**
**15.2**
$C_s$ $^1$A′

**C-05**
**15.7**
$C_1$ $^1$A

**C-06**
**16.2**
$C_s$ $^1$A′

**C-07**
**16.2**
$C_s$ $^1$A′

**C-08**
**17.8**
$C_1$ $^1$A

**C-09**
**18.6**
$C_s$ $^1$A′

**C-10**
**20.4**
$C_1$ $^1$A

***Figure 19**. Ten lowest-lying energy structures for $C_3H_3Li_3$ stoichiometry. The relative energies are given by the bolded blue values (singlets) in kcal/mol. Relative energies are at the TPSS+D3(BJ)/def2-TZVP level of theory including the zero-point energy (ZPE) corrections.*

### ***$C_6H_2Li_4$ stoichiometry***

The global minimum for such stoichiometry is **D-01** with $C_s$ symmetry, where the two organic fragments share all four lithium atoms in common. The calculated C-C bond for the $C_2^{2-}$ fragment is 1.259 Å, where its WBI indicates a carbon triple bond (2.935). The distances for the C-C bond is in excellent agreement with the reported 1.258 Å by Moreno et al.[36] for the monomer $C_2Li_2$. The presence of smaller organolithium fragments is not uncommon, Lagow has shown that pyrolysis of lithium compounds will lead to cleavage of C-C bonds by insertion of lithium atoms and the formation of smaller organic fragments, which eventually end in $C_2Li_2$ units.[1] On the other hand, the calculated C-C bonds for the $C_4H_2^{2-}$ are 1.248 Å for C4-C3 (WBI = 2.740), 1.441 Å for C3-C2 (WBI = 1.441) and 1.370 Å for C2-C1 (WBI = 1.860). The central C-Li bonds are longer (2.205 - 2.394 Å) than the perimeter ones (1.971 - 2.026 Å) and their WBI suggest that the central bonds have more ionic character (less than 0.100) than the perimeter ones (0.101 and 0.114). The computed NPA charges at the central and perimeter lithiums are +0.86 and +0.88 ~ +0.89 |e⁻|, respectively (**Figure 20**).

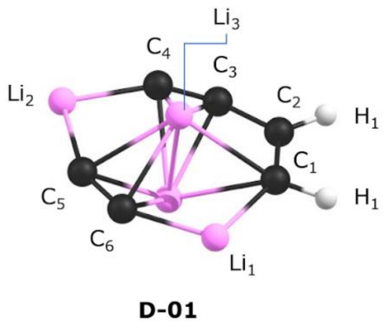

**D-01**

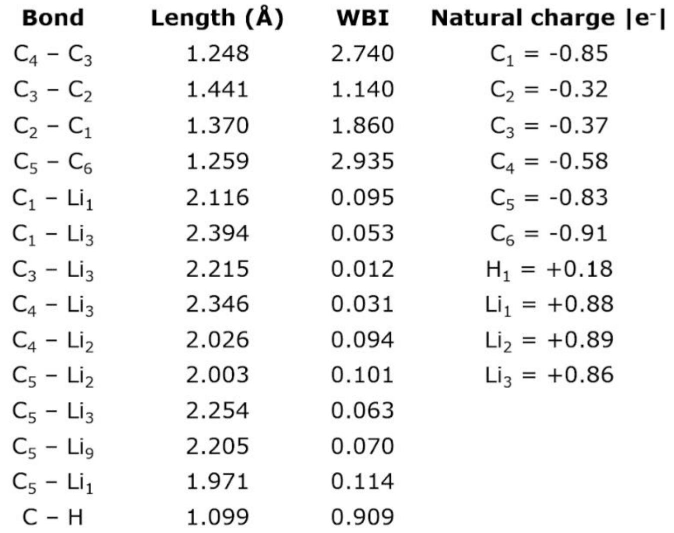

| Bond | Length (Å) | WBI | Natural charge \|e⁻\| |
|---|---|---|---|
| $C_4 - C_3$ | 1.248 | 2.740 | $C_1$ = -0.85 |
| $C_3 - C_2$ | 1.441 | 1.140 | $C_2$ = -0.32 |
| $C_2 - C_1$ | 1.370 | 1.860 | $C_3$ = -0.37 |
| $C_5 - C_6$ | 1.259 | 2.935 | $C_4$ = -0.58 |
| $C_1 - Li_1$ | 2.116 | 0.095 | $C_5$ = -0.83 |
| $C_1 - Li_3$ | 2.394 | 0.053 | $C_6$ = -0.91 |
| $C_3 - Li_3$ | 2.215 | 0.012 | $H_1$ = +0.18 |
| $C_4 - Li_3$ | 2.346 | 0.031 | $Li_1$ = +0.88 |
| $C_4 - Li_2$ | 2.026 | 0.094 | $Li_2$ = +0.89 |
| $C_5 - Li_2$ | 2.003 | 0.101 | $Li_3$ = +0.86 |
| $C_5 - Li_3$ | 2.254 | 0.063 | |
| $C_5 - Li_9$ | 2.205 | 0.070 | |
| $C_5 - Li_1$ | 1.971 | 0.114 | |
| C – H | 1.099 | 0.909 | |

***Figure 20****. Bond lengths (Å), Wiberg bond index and NPA charges |e⁻| of D-01 for $C_6H_2Li_4$ stoichiometry.*

The AdNDP analysis indicates the presence of four electron pairs (ON = 1.85 |e⁻|) localized at C1, C4, C5 and C6; four C-C σ-bonds (ON = 1.98 |e⁻|), two C-H σ-bonds (ON = 1.96 |e⁻|), three C-C π-bonds (ON = 1.92 |e⁻|), and two C-C π-bonds (ON = 1.95 |e⁻|). Therefore, we can visualize **D-01** as $C_2Li_2$ and $C_4H_2Li_2$ units, in which each of the bridging lithium atoms links carbon atoms from the other organic fragment (**Figure 21**).

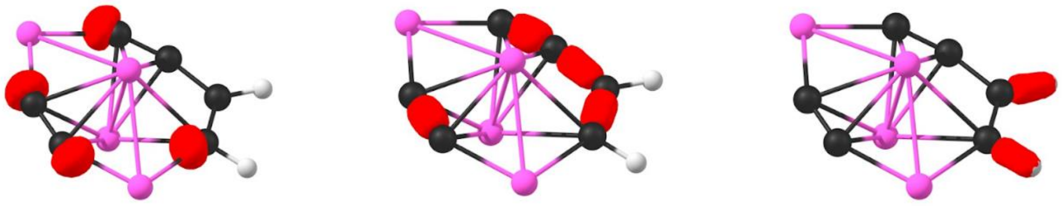

4 x 1c-2e electron pairs
ON = 1.85 $|e^-|$

4 x 2c-2e C-C $\sigma$-bonds
ON = 1.98 $|e^-|$

2 x 2c-2e C-H $\sigma$-bonds
ON = 1.96 $|e^-|$

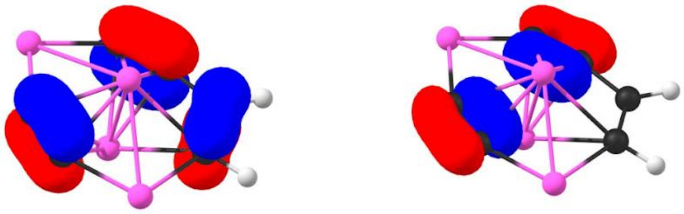

3 x 2c-2e $\pi$-bonds
ON = 1.92 $|e^-|$

2 x 2c-2e $\pi$-bonds
ON = 1.95 $|e^-|$

***Figure 21**. AdNDP analysis for **D-01** (ON is the occupation number).*

The **D-02** structure is a slightly higher-energy isomer of **D-01** located at 2.1 kcal/mol (at CCSD(T)/def2-TZVP level) above the global minimum. This structure can be obtained from **D-01** by rotating the $C_2Li_2$ unit and redistributing the remaining lithium atoms, while retaining the $C_s$ symmetry (**Figure 22**). The C-C bonds for the $C_2^{2-}$ fragment (1.260 Å, WBI = 2.969) and for the $C_4H_2^{2-}$ fragment (1.249, 1.445 and 1.375 Å; WBI = 2.745, 1.141 and 1.853, respectively) practically are the same to those in the previous one. The C-Li bonds are longer for the central lithiums (2.158 - 2.456 Å) than for the perimeter ones (2.048 - 2.161 Å), where the WBI are less than 0.100 and in the range of 0.100 to 0.114, respectively. The charges are -0.85 $|e^-|$ for C1 and C5, and -0.56 $|e^-|$ for C4, instead for the central lithiums are +0.87 $|e^-|$, and +0.85 and +0.87 $|e^-|$ for the perimeter ones. These results indicate that the overall charge transfer from the lithium atoms to the carbons in the organic fragments increases from **D-01** to **D-02**.

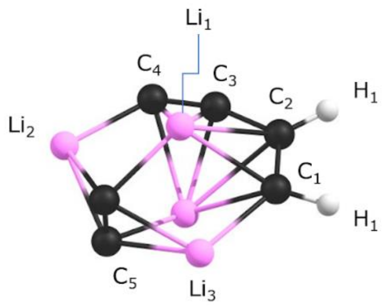

**D-02**

| Bond | Length (Å) | WBI | Natural charge \|e⁻\| |
|---|---|---|---|
| $C_4 - C_3$ | 1.249 | 2.745 | $C_1$ = -0.85 |
| $C_3 - C_2$ | 1.445 | 1.141 | $C_2$ = -0.34 |
| $C_2 - C_1$ | 1.375 | 1.853 | $C_3$ = -0.39 |
| $C_5 - C_5$ | 1.260 | 2.969 | $C_4$ = -0.56 |
| $C_1 - Li_1$ | 2.316 | 0.053 | $C_5$ = -0.85 |
| $C_1 - Li_2$ | 2.161 | 0.114 | $H_1$ = +0.18 |
| $C_2 - Li_1$ | 2.456 | 0.013 | $Li_1$ = +0.87 |
| $C_3 - Li_1$ | 2.158 | 0.012 | $Li_2$ = +0.85 |
| $C_4 - Li_1$ | 2.317 | 0.032 | $Li_3$ = +0.87 |
| $C_4 - Li_3$ | 2.048 | 0.100 | |
| $C_5 - Li_1$ | 2.068 | 0.110 | |
| $C_5 - Li_2$ | 2.126 | 0.071 | |
| $C_5 - Li_{11}$ | 2.169 | 0.063 | |
| C – H | 1.097 | 0.908 | |

***Figure 22**. Bond lengths (Å), Wiberg bond index and NPA charges |e⁻| of **D-02** for $C_6H_2Li_4$ stoichiometry.*

The third lowest-energy form is **D-03**. The energy difference between **D-03** and the global minimum is 7.3 kcal/mol (at CCSD(T)/def2-TZVP level). The C-C bond for the $C_2^{2-}$ fragment (1.261 Å, WBI = 2.932) does not change from the previous structures, but the $C_4H_2^{2-}$ fragment presents subtle changes (1.260, 1.428 and 1.355 Å; WBI = 2.645, 1.271 and 1.869, respectively). The central C-Li bonds are longer (2.144 - 2.265 Å) than the perimeter ones (2.048 - 2.216) but the overall WBI is less than 0.100 (**Figure 23**). The highest computed charges are in the $C_2^{2-}$ fragment (-0.90 and -0.85 |e⁻|), meanwhile for the $C_4H_2^{2-}$ are -0.65 and -0.66 |e⁻| at C3 and C5, respectively. The charges of the lithiums are in the range of +0.86 to +0.89 |e⁻|. In overall the charge transfer from the lithiums to the carbons are practically the same as in **D-01**.

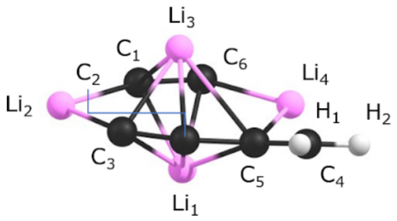

**D-03**

| Bond | Length (Å) | WBI | Natural charge \|e⁻\| |
|---|---|---|---|
| $C_5 - C_2$ | 1.260 | 2.645 | $C_1$ = -0.85 |
| $C_2 - C_3$ | 1.428 | 1.271 | $C_2$ = -0.39 |
| $C_3 - C_4$ | 1.355 | 1.869 | $C_3$ = -0.65 |
| $C_1 - C_6$ | 1.261 | 2.932 | $C_4$ = -0.37 |
| $C_1 - Li_2$ | 2.048 | 0.100 | $C_5$ = -0.66 |
| $C_1 - Li_3$ | 2.151 | 0.074 | $C_6$ = -0.90 |
| $C_1 - Li_1$ | 2.185 | 0.071 | H = +0.16 |
| $C_3 - Li_4$ | 2.216 | 0.080 | $Li_1$ = +0.86 |
| $C_3 - Li_1$ | 2.206 | 0.057 | $Li_2$ = +0.89 |
| $C_2 - Li_3$ | 2.144 | 0.014 | $Li_3$ = +0.87 |
| $C_2 - Li_1$ | 2.066 | 0.013 | $Li_4$ = +0.88 |
| $C_5 - Li_2$ | 2.053 | 0.097 | |
| $C_5 - Li_1$ | 2.265 | 0.037 | |
| $C_5 - Li_3$ | 2.209 | 0.046 | |
| C – H | 1.092 | 0.933 | |

***Figure 23**. Bond lengths (Å), Wiberg bond index and NPA charges |e⁻| of **D-03** for $C_6H_2Li_4$ stoichiometry.*

Increasing the degree of lithium substitution in benzene leads to further fragmentation instead to classical forms accordingly to our results (**Figure 24**). Although the lowest-lying energy structures are composed of $C_4H_2^{2-}$ and $C_2^{2-}$ fragments, most of the geometries present $C_2H^-$ and $C_2^{2-}$ fragments. Arrangements of $C_3H^{2-}$ fragments were also found but they correspond to high energy triplet structures (See supplementary section).

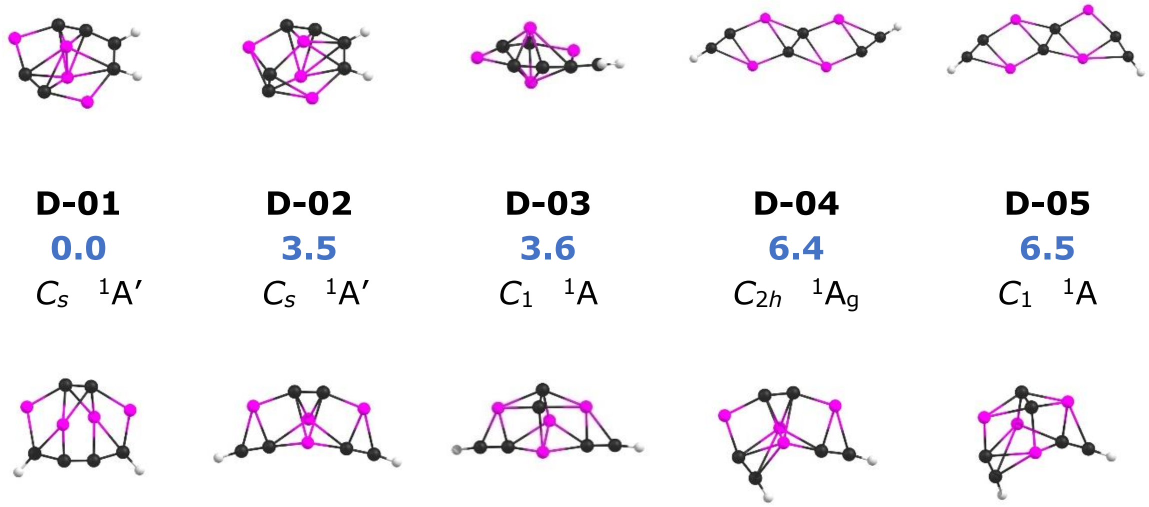

**D-01**
**0.0**
$C_s$ $^1A'$

**D-02**
**3.5**
$C_s$ $^1A'$

**D-03**
**3.6**
$C_1$ $^1A$

**D-04**
**6.4**
$C_{2h}$ $^1A_g$

**D-05**
**6.5**
$C_1$ $^1A$

**D-06**
**8.6**
$C_2$ $^1A$

**D-07**
**9.0**
$C_{2v}$ $^1A_1$

**D-08**
**9.0**
$C_{2v}$ $^1A_1$

**D-09**
**9.3**
$C_s$ $^1A'$

**D-10**
**9.3**
$C_1$ $^1A$

***Figure 24**. Ten lowest-lying energy structures for $C_6H_2Li_4$ stoichiometry. The relative energies are given by the bolded blue values (singlets) in kcal/mol. Relative energies are at the TPSS+D3(BJ)/def2-TZVP level, including the zero-point energy (ZPE) corrections.*

### *$C_6HLi_5$ stoichiometry*

The **E-01** structure was found as the global minimum for this system. It is composed of two $C_2^{2-}$ and one $C_2H^-$ fragments sharing all five lithium atoms in common. The calculated C-C bonds for $C_2^{2-}$ and $C_2H^-$ are 1.257 and 1.234 Å, respectively. Their WBI (2.961 - 2.964) indicates a carbon triple bond (**Figure 25**). The C-Li bonds are between 1.968 and 2.334 Å and most of them are ionic in nature (WBI 0.121 and below 0.100). The charges of both $C_2^{2-}$ fragments are -0.80 and -0.93 $|e^-|$, for the $C_2H^-$ fragment are -0.44 and -0.65 $|e^-|$, and for the lithiums are between +0.81 and +0.89 $|e^-|$.

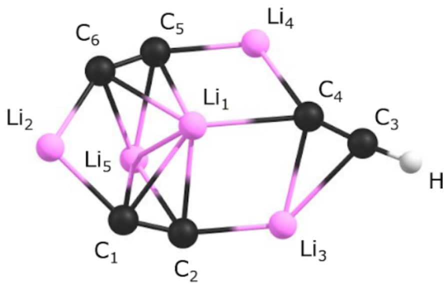

**E-01**

| Bond | Length (Å) | WBI | Natural charge $|e^-|$ |
|---|---|---|---|
| $C_1 - C_2$ | 1.257 | 2.961 | $C_1$ = -0.79 |
| $C_3 - C_4$ | 1.234 | 2.963 | $C_2$ = -0.93 |
| $C_5 - C_6$ | 1.257 | 2.964 | $C_3$ = -0.44 |
| $C_1 - Li_1$ | 2.311 | 0.054 | $C_4$ = -0.65 |
| $C_1 - Li_2$ | 2.035 | 0.097 | $C_5$ = -0.93 |
| $C_1 - Li_5$ | 2.152 | 0.067 | $C_6$ = -0.80 |
| $C_2 - Li_1$ | 2.220 | 0.064 | H = +0.23 |
| $C_2 - Li_3$ | 1.968 | 0.121 | $Li_1$ = +0.81 |
| $C_2 - Li_5$ | 2.228 | 0.068 | $Li_2$ = +0.89 |
| $C_3 - Li_3$ | 2.334 | 0.022 | $Li_3$ = +0.89 |
| $C_4 - Li_3$ | 2.202 | 0.051 | $Li_4$ = +0.89 |
| $C_4 - Li_4$ | 2.093 | 0.085 | $Li_5$ = +0.84 |
| C – H | 1.072 | 0.916 | |

***Figure 25**. Bond lengths (Å), Wiberg bond index and NPA charges $|e^-|$ of **E-01** for $C_6HLi_5$ stoichiometry.*

The AdNDP analysis shows five electron pairs (ON = 1.86 $|e^-|$) localized at C1, C2, C4, C5 and C6; three C-C σ-bonds (ON = 1.99 $|e^-|$), one C-H σ-bond (ON = 1.99 $|e^-|$), and six C-C π-bonds (ON = 1.97 $|e^-|$). Thus **E-01** structure can be understood as two $C_2Li_2$ units sharing both lithiums with $Li^+$ cations that connect both $C_2Li_2$ with the $C_2HLi$ fragment (**Figure 26**).

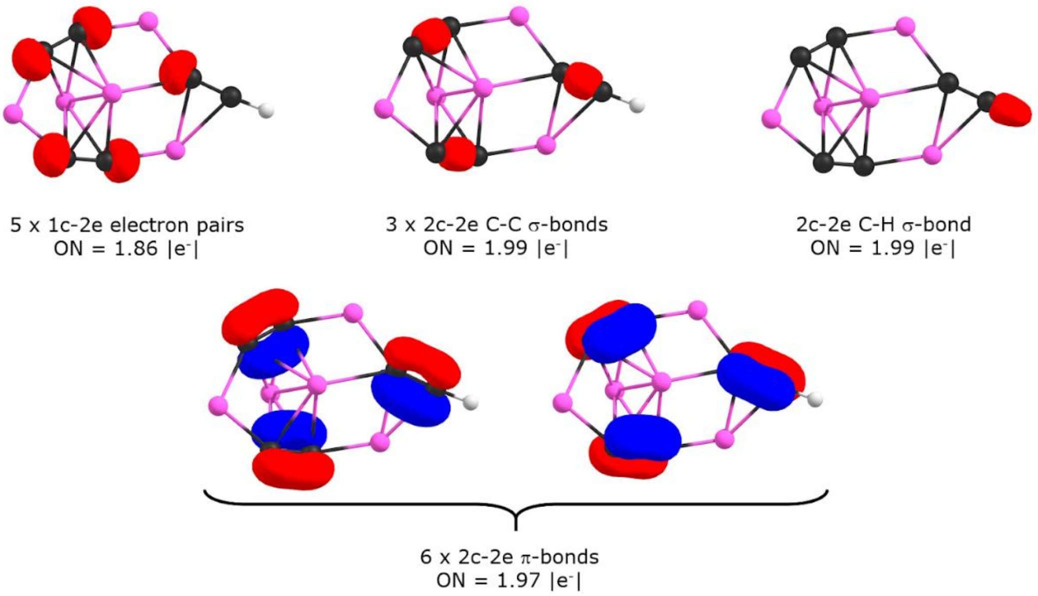

5 x 1c-2e electron pairs
ON = 1.86 $|e^-|$

3 x 2c-2e C-C $\sigma$-bonds
ON = 1.99 $|e^-|$

2c-2e C-H $\sigma$-bond
ON = 1.99 $|e^-|$

6 x 2c-2e $\pi$-bonds
ON = 1.97 $|e^-|$

***Figure 26.*** *AdNDP analysis for **E-01** (ON is the occupation number).*

The isomer **E-02** is located 3.01 kcal/mol (at CCSD(T)/def2-TZVP level) above the global minimum. This structure can be obtained from **E-01** by rotating one $C_2Li_2$ unit and redistributing the remaining lithium atoms (**Figure 27**). The C-C bonds for both $C_2^{2-}$ fragments and for the $C_2H^-$ fragment basically are the same to those in the previous structure. The C-Li bonds are between 1.974 and 2.331 Å, their WBI suggests that most of them are basically ionic (0.117 and below 0.100). The charges for $C_2^{2-}$ fragments are slightly different: at C5 and C6 are -0.83 and -0.88 $|e^-|$, meanwhile at C3 and C4 are -0.92 and -0.79 $|e^-|$, respectively. For the $C_2H^-$ fragment are -0.45 and -0.65 $|e^-|$, and for the lithiums are between +0.80 and +0.89 $|e^-|$. These results indicate that the overall charge transfer from the lithium atoms to the carbons in the organic fragments decreases from **E-01** to **E-02**.

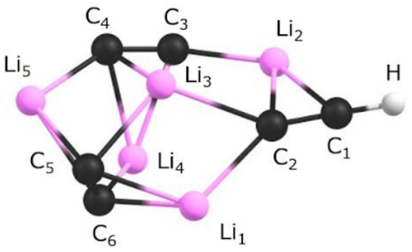

**E-02**

| Bond | Length (Å) | WBI | Natural charge $\|e^-\|$ |
|---|---|---|---|
| $C_2 - C_1$ | 1.235 | 2.957 | $C_1$ = -0.45 |
| $C_3 - C_4$ | 1.258 | 2.956 | $C_2$ = -0.65 |
| $C_5 - C_6$ | 1.260 | 2.968 | $C_3$ = -0.92 |
| $C_1 - Li_2$ | 2.331 | 0.022 | $C_4$ = -0.79 |
| $C_2 - Li_2$ | 2.217 | 0.048 | $C_5$ = -0.83 |
| $C_2 - Li_3$ | 2.222 | 0.092 | $C_6$ = -0.88 |
| $C_3 - Li_2$ | 1.974 | 0.117 | H = +0.23 |
| $C_3 - Li_3$ | 2.223 | 0.063 | $Li_1$ = +0.87 |
| $C_3 - Li_4$ | 2.194 | 0.072 | $Li_2$ = +0.89 |
| $C_4 - Li_3$ | 2.227 | 0.064 | $Li_3$ = +0.80 |
| $C_4 - Li_4$ | 2.149 | 0.065 | $Li_4$ = +0.86 |
| $C_5 - Li_5$ | 2.133 | 0.074 | $Li_5$ = +0.87 |
| $C_5 - Li_1$ | 2.093 | 0.078 | |
| C – H | 1.072 | 0.916 | |

***Figure 27**. Bond lengths (Å), Wiberg bond index and NPA charges $|e^-|$ of **E-02** for $C_6HLi_5$ stoichiometry.*

Our results indicate that the tendency to favor smaller fragments that lead to $C_2^{2-}$ carbanions is maintained (**Figure 28**). Besides several stable structures are hydride-type compounds and the triplets are located at relative energies above the 35 kcal/mol (see supplementary section).

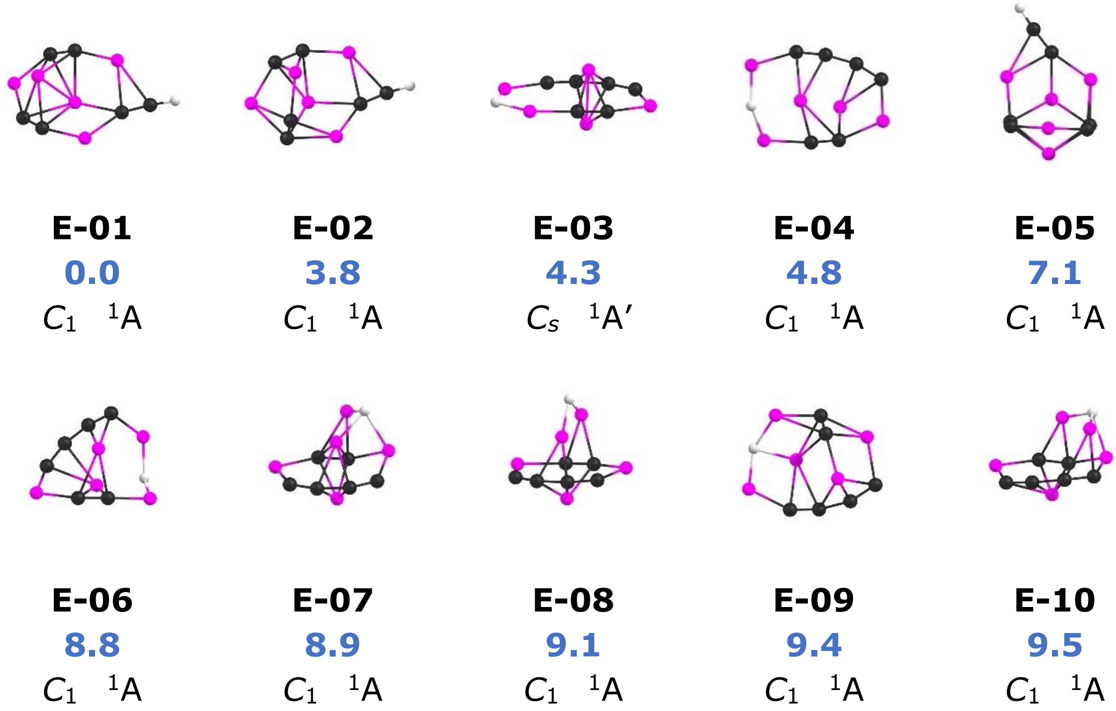

***Figure 28**. Ten Lowest-lying energy structures for $C_6HLi_5$ stoichiometry. The relative energies are given by the bolded blue values (singlets) in kcal/mol. Relative energies are at the TPSS+D3(BJ)/def2-TZVP level, including the zero-point energy (ZPE) corrections.*

### *$C_6Li_6$ stoichiometry*

In 1990, Baran and Lagow claimed the synthesis of hexalithiobenzene.[37,38] and assumed a benzene-like structure for this compound. Due to their inconclusive data about the $C_6Li_6$ structure, and scarce theoretical and experimental information, Xie and Schaefer decided to carry out a preliminary theoretical study of this molecule using ab initio quantum-mechanical methods.[38] They restricted the search just to those molecular structures in which the carbon atoms are arranged in ring or cages. From that work we can highlight two structures: a benzene-like and a star-like structure (**Figure 29**).

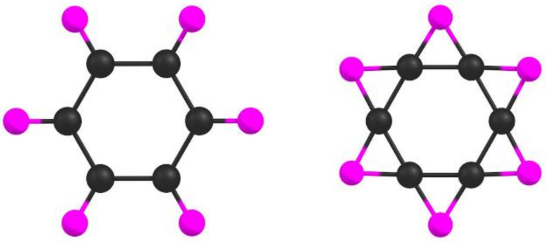

***Figure 29**. Benzene-like stationary point (left) and star-like structure (right) for $C_6Li_6$. The benzene-like structure lies 122 kcal/mol above the star-like structure.*

At first, it was assumed that the structure of $C_6Li_6$ should be similar to the benzene, but Xie found that it has several imaginary frequencies at MP2/TZP level of theory, which means this stationary point is a saddle point and not a stable structure. The star-like structure was studied because it is known that lithium prefers bridging positions, as has been reported for alkyl lithium compounds.[3] This $D_{6h}$ structure was located 122 kcal/mol below the benzene-like structure and compared with some acyclic $C_6Li_6$ structures, but still the star-like structure was below them.

Shortly after, Smith reported a structure of $C_6Li_6$ whose energy lies substantially lower than the star-like one using early DFT methods.[39] Smith re-examined the previous structures and extended the search to include tightly clustered trimmers of $C_2Li_2$ units. With this approach, Smith was able to find several structures whose energy lies appreciably lower than that of the star-like structure. Among them, the lowest energy (80 kcal/mol below the star-like structure) is a $D_3$ symmetry structure, where each lithium connects carbon atoms of another $C_2Li_2$ unit.

In 2013, the group of Merino carried out an exhaustive examination of the $C_6Li_6$ PES using a genetic algorithm,[36] in which some of us reported a new asymmetrical minimum whose energy is 6 kcal/mol lower than the $D_3$ structure (**Figure 30**).

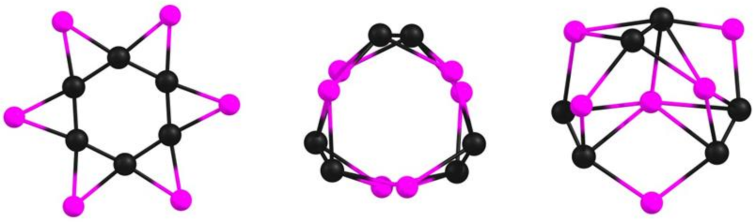

***Figure 30****. Low-lying structures of $C_6Li_6$. From left to right their relative energies (at CCSD(T)/def2-TZVP level) are 82.9, 6.3 and 0.0 kcal/mol.*[36]

Our results support that the minimum suggested by Moreno et al. (**F-01**) is the most stable one for this stoichiometry. The calculated C-C (1.258 - 1.260 Å, WBI = 2.958 - 2.943) and C-Li bonds (2.030 - 2.233 Å, WBI less than 0.100 threshold) are in excellent agreement with what been already reported (**Figure 31**).[36] The computed NPA charges for the carbons are in the range of -0.83 to -0.89 $|e^-|$, and for the lithium atoms are between +0.85 and +0.89 $|e^-|$ except for Li6, which has a significant lower charge (+0.78 $|e^-|$)

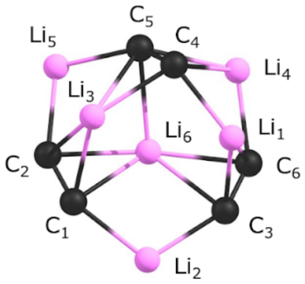

**F-01**

| **Bond** | **Length (Å)** | **WBI** | **Natural charge \|e$^-$\|** |
|---|---|---|---|
| $C_2 - C_1$ | 1.258 | 2.958 | $C_1 = -0.83$ |
| $C_3 - C_6$ | 1.259 | 2.950 | $C_2 = -0.88$ |
| $C_4 - C_5$ | 1.260 | 2.943 | $C_3 = -0.84$ |
| $C_2 - Li_3$ | 2.090 | 0.077 | $C_4 = -0.89$ |
| $C_2 - Li_6$ | 2.233 | 0.065 | $C_5 = -0.85$ |
| $C_2 - Li_5$ | 2.030 | 0.098 | $C_6 = -0.87$ |
| $C_1 - Li_3$ | 2.216 | 0.073 | $Li_1 = +0.86$ |
| $C_1 - Li_6$ | 2.177 | 0.072 | $Li_2 = +0.88$ |
| $C_1 - Li_2$ | 2.044 | 0.104 | $Li_3 = +0.85$ |
| $C_3 - Li_1$ | 2.168 | 0.075 | $Li_4 = +0.88$ |
| $C_3 - Li_6$ | 2.199 | 0.071 | $Li_5 = +0.89$ |
| $C_3 - Li_2$ | 2.048 | 0.103 | $Li_6 = +0.78$ |

***Figure 31****. Bond lengths (Å), Wiberg bond index and NPA charges |e$^-$| of* ***F-01*** *for $C_6Li_6$ stoichiometry.*

The AdNDP analysis shows six electron pairs (ON = 1.86 |e$^-$|) localized at the carbon atoms; three C-C σ-bonds (ON = 1.99 |e$^-$|), and six C-C π-bonds (ON = 1.97 |e$^-$|). Therefore **F-01** structure can be visualized as three $C_2Li_2$ units sharing lithiums in common (**Figure 32**).

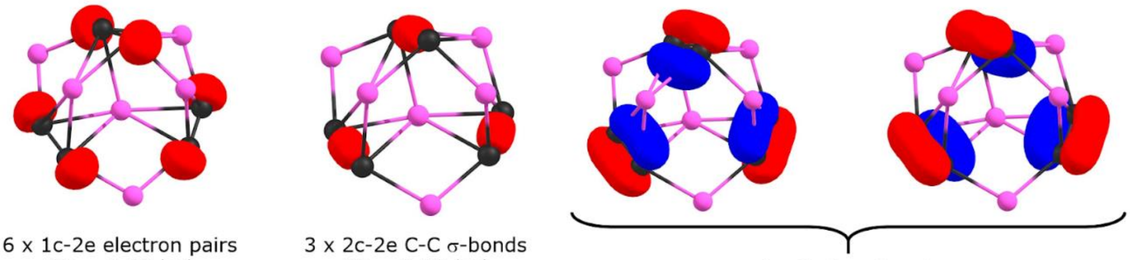

6 x 1c-2e electron pairs
ON = 1.86 |e$^-$|

3 x 2c-2e C-C σ-bonds
ON = 1.99 |e$^-$|

6 x 2c-2e π-bonds
ON = 1.97 |e$^-$|

***Figure 32****. AdNDP analysis for* ***F-01*** *(ON is the occupation number).*

The second lowest-lying energy structure is **F-02**, this form adopts a $D_3$ symmetry and is located 6.3 kcal/mol (at CCSD(T)/def2-TZVP level) above the global minimum (**Figure 33**). All C-C bonds have the same length (1.258 Å) whereas two kinds of C-Li bonds can be distinguished: the shorter 2.045 Å corresponds to the distance from the lithium of one $C_2Li_2$ unit to the carbon of another unit; and the longer ones (2.146 and 2.180 Å) that correspond to the distance from the lithium atoms to the carbon within the $C_2Li_2$ unit. The WBI for C-C and C-Li bonds are 2.977 and less than 0.100, respectively. Which suggests the important ionic character of the C-Li bonds. The NPA charges at carbons and lithiums are ±0.85 $|e^-|$, respectively. Which corroborates the ionic nature of the organolithium bonds. These results are in excellent agreement with what have been reported by Smith and Moreno.[36,39]

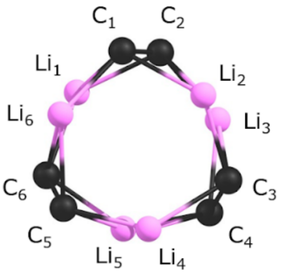

**F-02**

| **Bond** | **Length (Å)** | **WBI** | **Natural charge $\|e^-\|$** |
|---|---|---|---|
| C – C | 1.258 | 2.977 | C = -0.85 |
| $C_2$ – $Li_1$ | 2.146 | 0.077 | Li = +0.85 |
| $C_2$ – $Li_2$ | 2.180 | 0.058 | |
| $C_2$ – $Li_3$ | 2.049 | 0.015 | |

***Figure 33****. Bond lengths (Å), Wiberg bond index and NPA charges $|e^-|$ of* ***F-02*** *for $C_6Li_6$ stoichiometry.*

**F-03** is the third lowest-lying energy form, whose calculated relative energy is 8.1 kcal/mol (at CCSD(T)/def2-TZVP level) with respect to the global minimum. It is composed of three $C_2Li_2$ units sharing several lithium atoms in common, in such a shape that reminiscences of a bell with $C_s$ symmetry. All the C-C bonds are virtually the same (1.257 and 1.259 Å) with WBI of 2.960, indicating carbon triple bonds (**Figure 34**). The Li4 and Li5 present the shorter C-Li bonds (2.014 and 1.978 Å, WBI = 0.100 and 0.117, respectively) that connects two $C_2Li_2$ units, meanwhile the longer ones (2.014 - 2.412 Å) corresponds to the organolithium bonds within the $C_2Li_2$ unit. Their WBI for the longer C-Li bonds are less than 0.100, suggesting the predominant ionic character. The charges at C1, C2 and C3 are -0.81, -0.91 and -0.87 $|e^-|$, respectively; for the central lithiums the charge is slightly lower (+0.85 and +0.80 $|e^-|$) than the perimeter ones (+0.88 and +0.90 $|e^-|$). These results indicate that the overall charge transfer from the lithiums to the carbon fragments is maintained throughout all the previous structures.

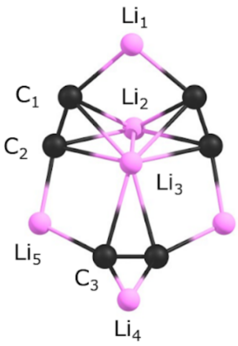

**F-03**

| Bond | Length (Å) | WBI | Natural charge $\|e^-\|$ |
|---|---|---|---|
| $C_1 - C_2$ | 1.257 | 2.960 | $C_1$ = -0.81 |
| $C_3 - C_3$ | 1.259 | 2.960 | $C_2$ = -0.91 |
| $C_1 - Li_1$ | 2.014 | 0.100 | $C_3$ = -0.87 |
| $C_1 - Li_2$ | 2.149 | 0.066 | $Li_1$ = +0.88 |
| $C_1 - Li_3$ | 2.412 | 0.049 | $Li_2$ = +0.85 |
| $C_2 - Li_2$ | 2.258 | 0.064 | $Li_3$ = +0.80 |
| $C_2 - Li_3$ | 2.263 | 0.067 | $Li_4$ = +0.90 |
| $C_2 - Li_5$ | 1.978 | 0.117 | $Li_5$ = +0.88 |
| $C_3 - Li_5$ | 2.036 | 0.093 | |
| $C_3 - Li_3$ | 2.374 | 0.052 | |
| $C_3 - Li_4$ | 2.014 | 0.091 | |
| $Li_2 - Li_3$ | 2.445 | 0.013 | |

***Figure 34****. Bond lengths (Å), Wiberg bond index and NPA charges $|e^-|$ of* ***F-03*** *for $C_6Li_6$ stoichiometry.*

The exploration found several minima where most of them are composed by $C_2Li_2$ units and tend to form cage-shaped geometries (**Figure 35**). The first triplet structure is located at 46.1 kcal/mol above the global minimum (see the supplementary section).

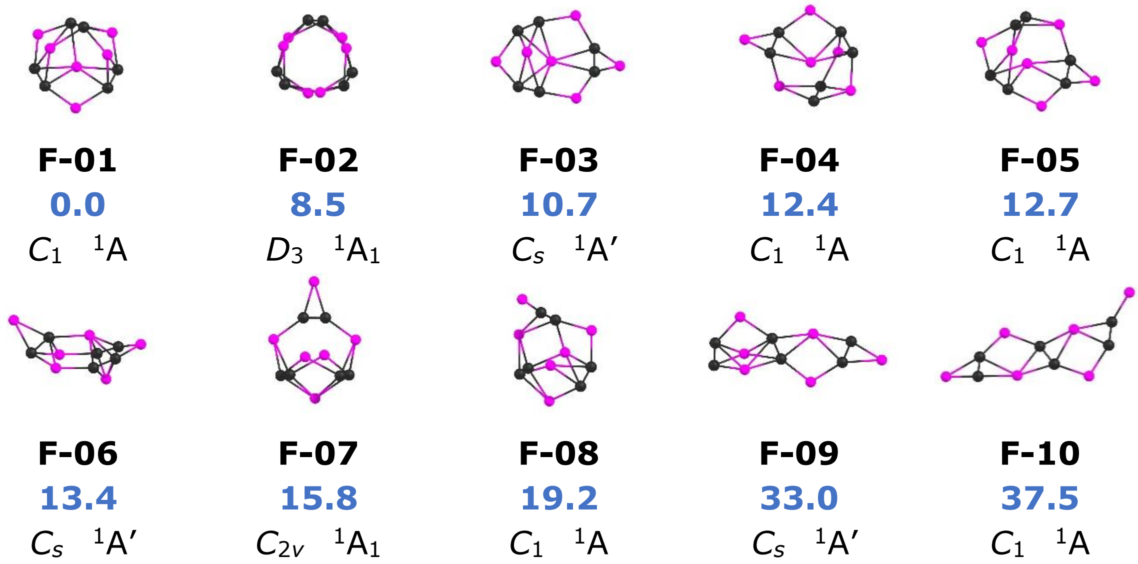

***Figure 35**. Ten Lowest-lying energy structures for $C_6Li_6$ stoichiometry. The relative energies are given by the bolded blue values (singlets) in kcal/mol. Relative energies are at the TPSS+D3(BJ)/def2-TZVP level, including the zero-point energy (ZPE) corrections.*

# Chapter 3. Hexaalkali stoichiometries

Organolithium compounds are widely used in organic synthesis due to their great versatility as key intermediaries in organic synthesis. They are more reactive than the typical Grignard reagents,[40] an excellent alkylation reagents, and are used as initiators for some economically important polymerizations (styrene, isoprene, butadiene, etc).[41–46] All these applications have shadowed the chemistry of organometallic compounds of the heavier alkali metals, since these compounds are difficult to isolate and present a high reactivity that make them unsuitable for being intermediaries in synthesis.[47] Information on the structure and bonding in alkali-metal species has been mainly focused on lithium derivatives, while the heavier analogues have dealt with limited extent. For example, in a 2004 review article,[48] a search in the Cambridge Structural Database (CSD) revealed 778 structures with a C-Li bond, 197 with a C-Na bond, 235 with a C-K bond, 57 with a C-Rb bond, and just 31 with a C-Cs bond. Interestingly, there are more reports about compounds with C-K bond than C-Na bond, despite the increasing reactivity of the compounds as descending the group of alkali-metals. As frequently observed potassium, rubidium, and cesium compounds display somewhat similar chemistry, which typically differs from that of the lithium and sodium analogues.

As mentioned before, the slow development of heavy alkali organometallic chemistry is due to high reactivity, as rationalized by the increase of polar character of the metal – ligand bond due to the reduced polarizing ability of the metals. The increase in ionic character on descending the group of alkali-metals is clearly indicated by the increase in ionic radii:

a) $Li^+$ (0.69 Å)
b) $Na^+$ (0.97 Å)
c) $K^+$ (1.33 Å)
d) $Rb^+$ (1.47 Å)
e) $Cs^+$ (1.67 Å)

Further information supporting the similarity of organolithium and sodium compounds is the structural data on the solvent-free $CH_3M$ (M = Li, Na). Using high-precision spectroscopy, a study revealed similar tetrahedral structures between the monomers of the methyl derivatives in gas phase, where they reported a 1.959 and 2.299 Å for the distances of C-Li and C-Na, respectively.[49] These data agree well with ab initio computations. Both $CH_3Na$ and $CH_3Li$ crystallize as tetramer, with the four metal atoms at the corners of a tetrahedral and the methyl groups capping the faces. Instead potassium, rubidium and cesium methyl derivatives adopt the ionic lattice of the NiAs structure, in which the methyl groups are surrounded in trigonal prismatic fashion by the alkali-metals, while the metal coordination spheres are comprised of an octahedral environment provided by six methyl groups.[50–52]

One of the most emblematic alkali organometallic compounds, due to their versatility and theory implications, is the alkali phenyl. The synthesis of $C_6H_5M$ (M = Li, Na, K, Rb, and Cs) were already reported,[53] but crystallographic and electronic data is scarce. That is why several theoretical studies proposed alkali-based structures to create new lines of investigation. Tang et al. conducted a generalized gradient approximation (GGA) DFT study of the structure, electronic properties, and hydrogen storage capabilities of alkali atom coated clusters $C_6M_6$ (M = Li and Na).[54] One of their conclusions was that the most stable site for the alkali-metal is to bridge the C-C bond and form the star-like structure, which seems unlikely based on the results discussed in the previous Chapter.

So, we decided to explore the PES of $C_6E_6$ systems (E = Na, K, Rb, Cs) and locate the most stable structures, not only ring-based ones but also clustered trimers of $C_2E_2$ units, or any other type.

### ***$C_6Na_6$ stoichiometry***

The three lowest-lying structures are similar to their lithium analogues. The **G-01** is located as the global minimum, then **G-02**, which adopts a *D*3 symmetry, and **G-03** are at 3.8 and 4.5 kcal/mol above (at CCSD(T)/def2-TZVP level), respectively. The calculated C-Na bonds are in the range of 2.419 - 2.700 Å (**Figure 36**). The WBI for all the C-Na bonds is less than 0.100 threshold, which indicates their ionic character. The presence of $C_2^{2-}$ fragments in the structures is confirmed by their C-C bonds (1.262 - 1.264 Å, WBI = 2.983 - 2.990).

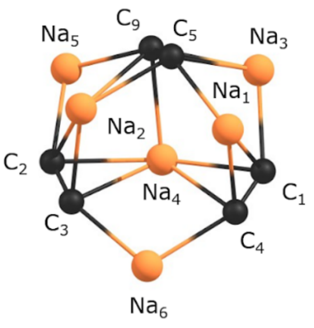

**G-01**

| Bond | Length (Å) | WBI | Natural charge \|e$^-$\| |
|---|---|---|---|
| C$_2$ – C$_3$ | 1.262 | 2.987 | C$_1$ = -0.84 |
| C$_4$ – C$_1$ | 1.263 | 2.983 | C$_2$ = -0.85 |
| C$_5$ – C$_6$ | 1.263 | 2.985 | C$_3$ = -0.84 |
| C$_2$ – Na$_2$ | 2.448 | 0.080 | C$_4$ = -0.85 |
| C$_2$ – Na$_4$ | 2.578 | 0.063 | C$_5$ = -0.86 |
| C$_2$ – Na$_5$ | 2.399 | 0.111 | C$_6$ = -0.86 |
| C$_3$ – Na$_2$ | 2.515 | 0.083 | Na$_1$ = +0.85 |
| C$_3$ – Na$_4$ | 2.532 | 0.066 | Na$_2$ = +0.84 |
| C$_3$ – Na$_6$ | 2.419 | 0.106 | Na$_3$ = +0.87 |
| C$_4$ – Na$_1$ | 2.474 | 0.087 | Na$_4$ = +0.79 |
| C$_4$ – Na$_4$ | 2.534 | 0.067 | Na$_5$ = +0.88 |
| C$_4$ – Na$_6$ | 2.427 | 0.104 | Na$_6$ = +0.87 |

***Figure 36**. Bond lengths (Å), Wiberg bond index and NPA charges |e$^-$| of **G-01** for $C_6Na_6$ stoichiometry.*

The AdNDP analysis shows six electron pairs (ON = 1.77 |e$^-$|) localized at the carbon atoms; three C-C σ-bonds (ON = 1.99 |e$^-$|), and six C-C π-bonds (ON = 1.96 |e$^-$|). This data shows that **G-01** has similar bonding as in **F-01** (**Figure 37**).

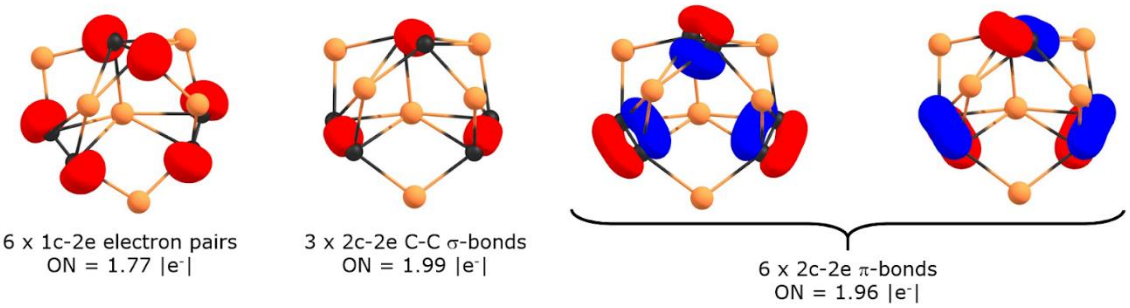
6 x 1c-2e electron pairs
ON = 1.77 |e$^-$|

3 x 2c-2e C-C σ-bonds
ON = 1.99 |e$^-$|

6 x 2c-2e π-bonds
ON = 1.96 |e$^-$|

***Figure 37**. AdNDP analysis for **G-01** (ON is the occupation number).*

The computed NPA charges for **G-01** and **G-02** are: at the carbons between -0.84 and -0.86 |e$^-$|, and at the sodium atoms +0.84 and +0.88 |e$^-$| except for Na4 in **G-01**, which is lower (+0.79 |e$^-$|). Both structures (**G-01** and **G-02**) have similar C-C bonds and charges as those in **F-01** and **F-02**, respectively (**Figure 38**). Given the larger size of sodium, the C-E distances are different to the lithium structures, nevertheless both lithium and sodium transfer virtually all their charge to the skeletal carbons.

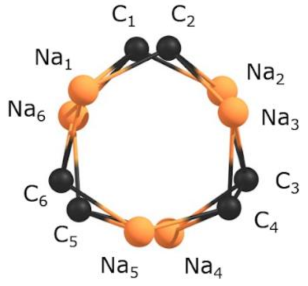

**G-02**

| Bond | Length (Å) | WBI | Natural charge \|e⁻\| |
|---|---|---|---|
| C – C | 1.263 | 2.990 | C = -0.85 |
| $C_2$ – $Na_1$ | 2.468 | 0.081 | Na = +0.85 |
| $C_2$ – $Na_2$ | 2.524 | 0.064 | |
| $C_2$ – $Na_3$ | 2.415 | 0.108 | |

***Figure 38**. Bond lengths (Å), Wiberg bond index and NPA charges |e⁻| of **G-02** for $C_6Na_6$ stoichiometry.*

The **G-03** structure can be obtained from **G-01** by rotating one $C_2^{2-}$ unit and redistributing all the sodium atoms. Such rotation does not affect the overall charge transfer from the sodium atoms to the carbons in $C_2^{2-}$ units. Such structure is unique to the $C_6Na_6$ stoichiometry given that the longer C-Na distance can help to overcome the electrostatic repulsion between the $Na^+$ cations (**Figure 39**).

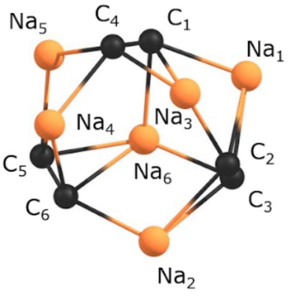

**G-03**

| Bond | Length (Å) | WBI | Natural charge \|e⁻\| |
|---|---|---|---|
| $C_1$ – $C_4$ | 1.264 | 2.983 | $C_1$ = -0.84 |
| $C_2$ – $C_3$ | 1.264 | 2.986 | $C_2$ = -0.87 |
| $C_5$ – $C_6$ | 1.264 | 2.984 | $C_3$ = -0.82 |
| $C_1$ – $Na_1$ | 2.498 | 0.083 | $C_4$ = -0.88 |
| $C_1$ – $Na_3$ | 2.636 | 0.049 | $C_5$ = -0.84 |
| $C_1$ – $Na_5$ | 2.700 | 0.047 | $C_6$ = -0.84 |
| $C_1$ – $Na_6$ | 2.624 | 0.055 | $Na_1$ = +0.87 |
| $C_2$ – $Na_1$ | 2.602 | 0.057 | $Na_2$ = +0.86 |
| $C_2$ – $Na_2$ | 2.594 | 0.061 | $Na_3$ = +0.85 |
| $C_2$ – $Na_3$ | 2.356 | 0.122 | $Na_4$ = +0.85 |
| $C_4$ – $Na_4$ | 2.479 | 0.086 | $Na_5$ = +0.87 |
| $C_4$ – $Na_5$ | 2.486 | 0.062 | $Na_6$ = +0.80 |

***Figure 39**. Bond lengths (Å), Wiberg bond index and NPA charges |e⁻| of **G-03** for $C_6Na_6$ stoichiometry.*

Most of the lower-lying structures (up to 7 kcal/mol) have the same geometry as their lithium counterparts. I. e. **G-04** and **F-07** both adopt $C_{2v}$

symmetry and the same shape, and only differ their C-E distances. At higher energies (above 7 kcal/mol) new geometries appear, like **G-09** which presents Na-Na bonds and the possible presence of a natride ($Na^-$) anion (**Figure 40**). Another important difference is the lower relative energies for triplet structures, where the first triplet (**G-33**) is located at 17.7 kcal/mol above the global minimum. Instead the first triplet for C6Li6 stoichiometry (**F-12**) is located at 46.1 kcal/mol (see supplementary section).

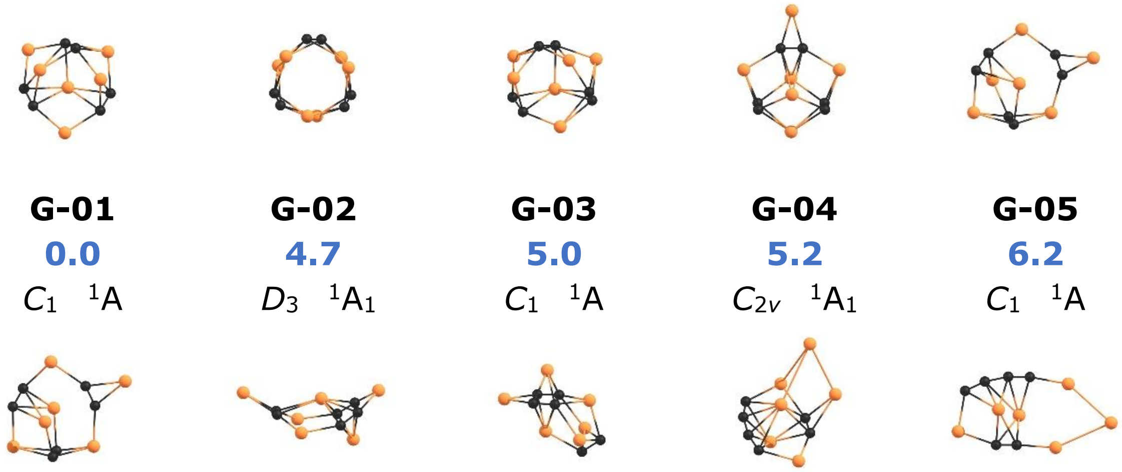

**G-01** **0.0** $C_1$ $^1A$

**G-02** **4.7** $D_3$ $^1A_1$

**G-03** **5.0** $C_1$ $^1A$

**G-04** **5.2** $C_{2v}$ $^1A_1$

**G-05** **6.2** $C_1$ $^1A$

**G-06** **6.8** $C_s$ $^1A'$

**G-07** **6.9** $C_s$ $^1A'$

**G-08** **7.2** $C_s$ $^1A'$

**G-09** **7.2** $C_1$ $^1A$

**G-10** **7.3** $C_1$ $^1A$

***Figure 40***. *Ten lowest-lying energy structures for $C_6Na_6$ stoichiometry. The relative energies are given by the bolded blue values (singlets) in kcal/mol. Relative energies are at the TPSS+D3(BJ)/def2-TZVP level, including the zero-point energy (ZPE) corrections.*

### ***$C_6E_6$ (E = K - Cs) stoichiometries***

Unlike the lighter alkali metal stoichiometries, the heavier ones exhibit different structures (**Figure 41**). These systems present similar arrangements for their three lowest-energy structures, most of them are alkalide-type arrangements, and their triplets are close to the global minimum (below 5 kcal/mol).

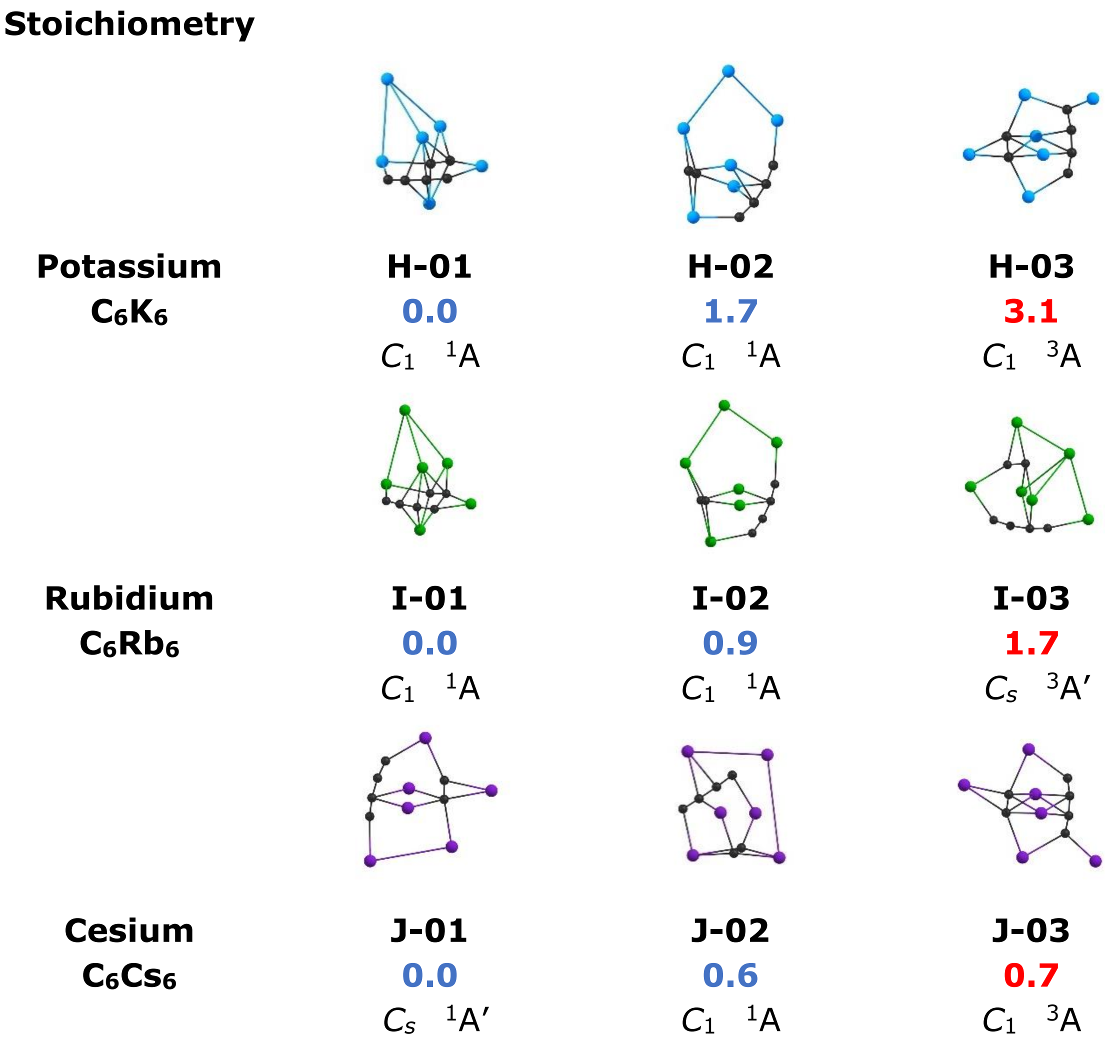

***Figure 41****. Three lowest-lying energy structures for the $C_6E_6$ stoichiometries (E = K – Cs). The relative energies are given by the* ***bolded blue (singlets)*** *and* ***red values (triplets)*** *in kcal/mol. Relative energies are at the TPSS+D3(BJ)/def2-TZVP level, including the zero-point energy (ZPE) corrections.*

The previous structures are composed of two dianionic fragments: $C_2^{2-}$ and $C_4^{2-}$, where four metallic cations bridge and link each fragment. Due to having more metallic atoms than the necessary to stabilize both organic fragments, some of them transfer part of their charge to another metallic atom, therefore stabilizing an alkalide-type ion ($E^-$) by metal-metal bonds. The computed NPA charges for $C_2^{2-}$ and $C_4^{2-}$ are in the ranges of [-1.70 to -1.87 $|e^-|$] and [-1.86 to -1.96 $|e^-|$], respectively. Throughout the lowest-lying energy structures of K, Rb and Cs stoichiometries, those fragments present the same data (**Table 1**).

***Table 1**. Bond lengths (Å), WBI and NPA charges of the organic fragments and alkali metal ions for the lowest-lying structures of the $C_6E_6$ stoichiometries (E = K - Cs).*

| | **Length (Å)** | **WBI** | **NPA charge $\|e^-\|$** |
|---|---|---|---|
| **$C_2^{2-}$ bond** | | | |
| C-C | 1.265 – 1.266 | 3.001 – 2.968 | -1.70 to -1.87 |
| **$C_4^{2-}$ bonds** | | | |
| $C_{term}$ – $C_{int}$ | 1.255 – 1.266 | 2.597 – 2.638 | -1.86 to -1.96 |
| $C_{int}$ – $C_{int}$ | 1.372 – 1.379 | 1.237 – 1.376 | |
| **C-E bonds** | | | **$E^+$** |
| C-K | 2.713 – 3.017 | < 0.100 | +0.57 to +0.93 |
| C-Rb | 2.873 – 3.117 | < 0.100 | +0.46 to +0.94 |
| C-Cs | 2.987 – 3.205 | < 0.100 | +0.57 to +0.95 |
| **E-E bonds** | | | **$E^-$** |
| K-K | 4.444 – 4.980 | 0.150 – 0.457 | -0.35 to -0.40 |
| Rb-Rb | 4.315 – 5.362 | 0.164 – 0.451 | -0.29 to -0.43 |
| Cs-Cs | 4.549 – 5.932 | 0.126 – 0.631 | -0.02 to -0.24 |

The shape and charges are independent of the nature of the alkali metal. The calculated NPA charges (+0.46 and +0.57 $|e^-|$ for K, Rb and Cs) indicate that the alkali metal atoms do not transfer all their charge to the skeletal carbons and the charge of the alkalide ion is roughly the same.

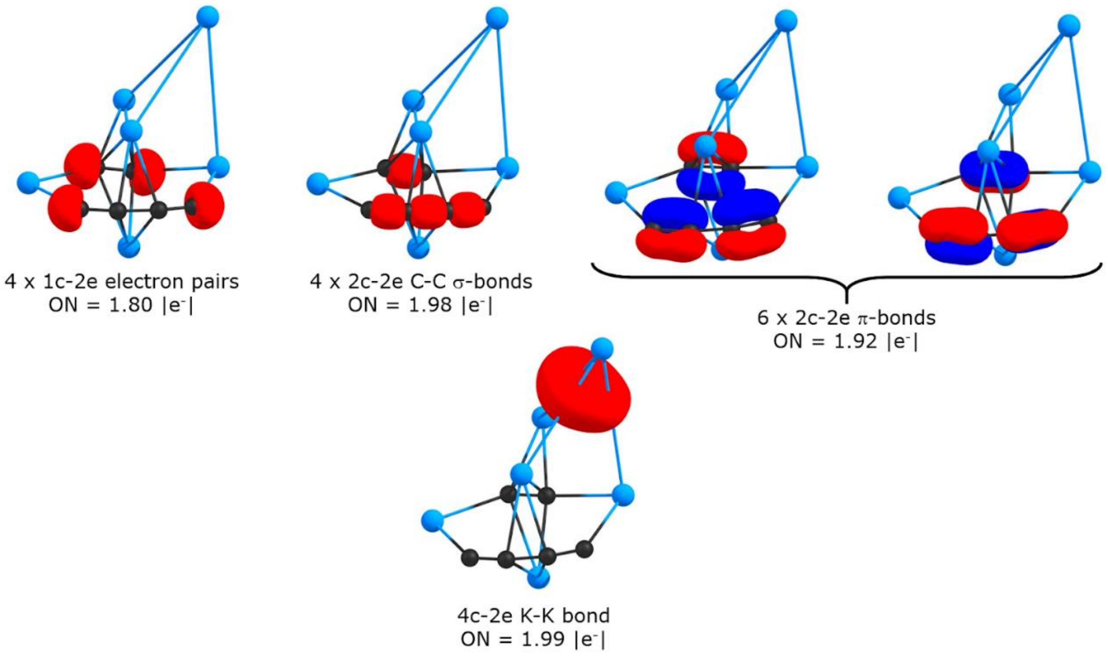

***Figure 42**. AdNDP analysis for **H-01** (ON is the occupation number).*

Our AdNDP analysis of **H-01** (**Figure 42**) shows four electron pairs with an occupation number (ON) of 1.80 $|e^-|$, four C-C σ-bonds (ON = 1.98 $|e^-|$), 6 C-C π-bonds (ON = 1.98 $|e^-|$), and one 4c-2e metallic bond (ON = 1.99 $|e^-|$). Same bonding and similar ONs were obtained also in the AdNDP analysis of **I-01**. In the case of **J-01** was not possible to perform an AdNDP analysis due to the *multifwn*[55] program cannot support f orbitals for the cesium atoms.

The **H-02** and **I-02** structures present the same geometry and similar relative energies with respect to their global minimum (1.4 and 0.9 kcal/mol at CCSD(T)/def2-TZVP for potassium and rubidium, respectively), where the $C_2^{2-}$ fragment is rotated circa 90° with respect to the plane formed by the $C_4^{2-}$ and several alkali metal atoms. Such arrangement increases the length of the E-E bonds and makes the alkalide ion pointing out of the plane. **J-02** structure is related to the previous geometry since $C_4^{2-}$ an extra C-Cs bond and pulls the alkalide ion closer to the organic fragment.

The heavier stoichiometries present triplet structures closer to the global minimum (3.7, 1.7 and 0.7 kcal/mol for first triplet of $C_6K_6$, $C_6Rb_6$ and $C_6Cs_6$ stoichiometries, respectively) (**Figure 43**). Arrangements with only $C_2^{2-}$ fragments are located at 5.5, 12.4 and 8.5 kcal/mol for **H-19**,

**I-22** and **J-22**, respectively. Analogues related to **F-01** were found for potassium (**H-35** at 9.3 kcal/mol), rubidium (**I-26** at 18.7 kcal/mol) and cesium (**J-32** at 16.3 kcal/mol) stoichiometries. Only a $D_3$ symmetry analogue to **F-02** was found within the 20 kcal/mol for the potassium molecular system (**H-52** at 13.2 kcal/mol) (see supplementary section).

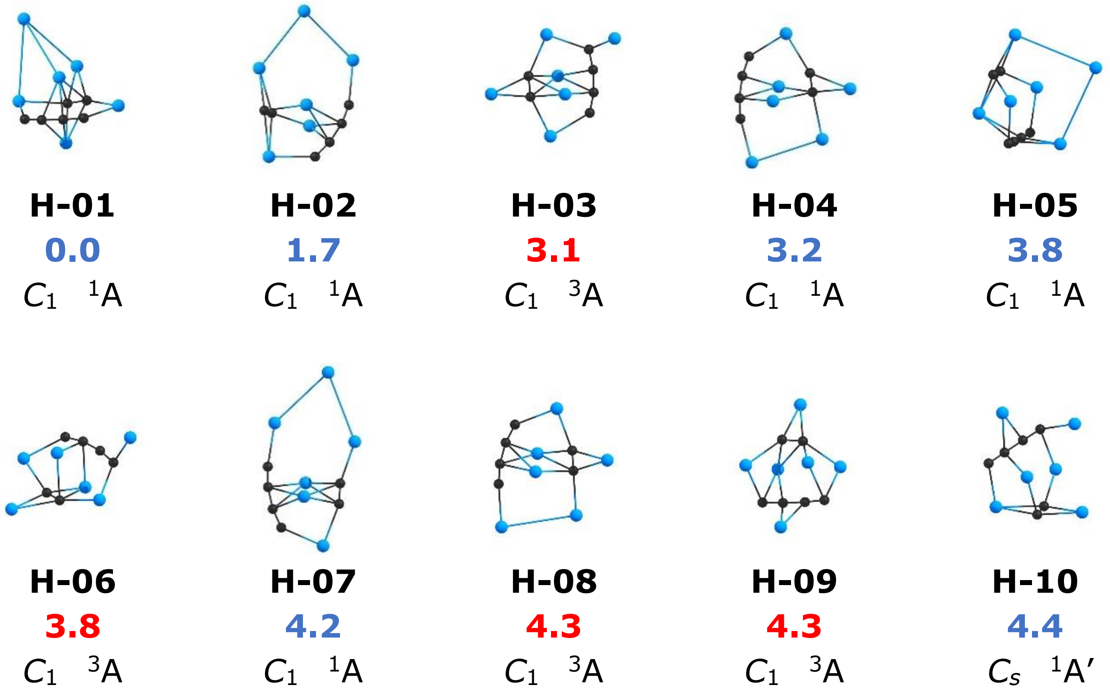

***Figure 43**. Ten lowest-lying energy structures for the $C_6K_6$ stoichiometry. The relative energies are given by the **bolded blue (singlets)** and **red values (triplets)** in kcal/mol. Relative energies are at the TPSS+D3(BJ)/def2-TZVP level, including the zero-point energy (ZPE) corrections.*

# Chapter 4. Conclusions

In this work the PESs of $C_6H_{6-n}Li_n$ (n = 1 - 6) and $C_6E_6$ (E = Li - Cs) stoichiometries were explored systematically using GLOMOS, where our results show that phenyllithium (**A-01**) as the global minimum for the $C_6H_5Li$ stoichiometry, which is in agreement with what have been already reported in the literature. The AdNDP analysis and computed NPA charges indicate that the aromaticity of the ring is not affected because the lone pair at the *ipso* carbon is perpendicular to the $\pi$-system, so this structure can be visualized as a $C_6H_5^-$ anion interacting with a $Li^+$ cation. For the $C_6H_4Li_2$ stoichiometry, we proposed a new global minimum (**B-01**) which is 4.4 kcal/mol (at CCSD(T)/def2-TZVP) below than the one reported by Bachrach et al. One of the lithium atoms in **B-01** structure bridge both carbon atoms with lone pairs, meanwhile the other lithium interacts with the $\pi$-cloud of the ring, hence stabilizing the $C_6H_4^{2-}$ anion. The lowest-lying energy structure **C-01** for $C_6H_3Li_3$ stoichiometry is interesting, not only because it is located 4.9 kcal/mol (at CCSD(T)/def2-TZVP) below the former global minimum, but also presents a $H^-$ anion. In this arrangement the lithium transfers virtually all their charge to the skeletal carbons, but a $C_6H_3^{3-}$ is not stable, thus the organic fragment redistributes their charge between $H^-$ and $C_6H_2^{2-}$ anions. As the rate of lithium substitution in the benzene increases (n = 4 - 6) the lithium atoms promote the cleavage of the C-C bonds that lead to the formation of $C_2H^-$ and $C_2^{2-}$ fragments, as can be seen in **D-01**, **E-01** and **F-01**, respectively.

On the other hand, the lowest-lying structures for $C_6Na_6$ stoichiometry have similar shapes and symmetries as those in the $C_6Li_6$ system, i. e. **G-01** has similar arrangement and charges as **F-01**. But for the heavier alkali $C_6E_6$ stoichiometries (E = K, Rb and Cs) the most stable structures present two dianions ($C_2^{2-}$ and $C_4^{2-}$) and an alkalide ion ($E^-$). One requirement for the alkali metal to transfer its charge to the carbon atom is to be in direct contact with the organic fragment, which both lithium and sodium meet due to their relative small ionic radii (0.69 and 0.97 Å, respectively) and the compact structures they adopt. Instead, the heavier alkali metals (K, Rb and Cs) have longer ionic radii (1.33, 1.47 and 1.67 Å, respectively) which make that only few of them close enough to transfer their charge to the carbon atoms and those who are further retain their charge and establish E-E metallic bonds. The AdNDP analysis and computed NPA charges corroborate the formation of $C_4^{2-}$ fragment and the stabilization of such $E^-$ anion.

Few DFT calculations for polylithiathed benzenes have been reported in the literature, but such studies are limited to benzene-shaped arrangements and classical structures. Therefore, in this work we proposed lower-lying energy structures than those reported for the $C_6H_{6-n}Li_n$ stoichiometries. Also, our results indicate that charge transfer between the sodium and lithium is practically the same, and the arrangements they present are similar, therefore sodium has a promising potential as an alternative for lithium ion batteries. So, the computations performed in this thesis are a milestone toward the possible application of sodium ions as a substitute in future battery generation. Also, we are interested in the chemistry and structures of $C_6H_{6-x}E_x$ stoichiometries (x = 1 - 6, E = Na - Cs) as possible substitutes as intermediaries in organic synthesis or as new materials for hydrogen storage.

# SUPPLEMENTARY INFORMATION

All the structures found in each exploration are showed next. The relative energies calculated at TPSS+D3(BJ)/def2-TZVP including the ZPE correction are given in bolded blue for singlets and red for triplets.

$C_6H_5Li$ stoichiometry

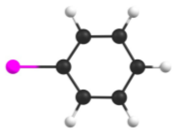

**A-01**
**0.0**
$C_{2v}$ $^{1}A_{1}$

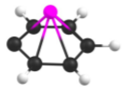

**A-02**
**11.6**
$C_s$ $^{1}A'$

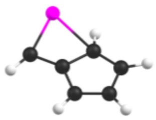

**A-03**
**26.0**
$C_1$ $^{1}A$

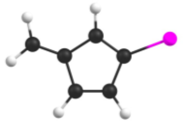

**A-04**
**29.8**
$C_s$ $^{1}A'$

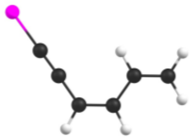

**A-05**
**36.2**
$C_s$ $^{1}A'$

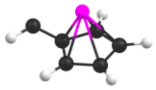

**A-06**
**37.4**
$C_1$ $^{1}A$

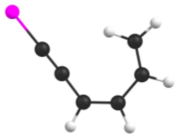

**A-07**
**39.2**
$C_s$ $^{1}A'$

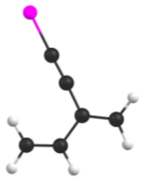

**A-08**
**39.3**
$C_s$ $^{1}A'$

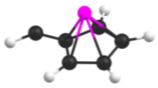

**A-09**
**41.2**
$C_1$ $^{3}A$

$C_6H_4Li_2$ stoichiometry

**B-01**
**0.0**
$C_s$ $^{1}A'$

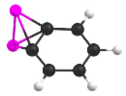

**B-02**
**3.1**
$C_{2v}$ $^{1}A_1$

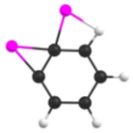

**B-03**
**4.9**
$C_s$ $^{1}A'$

**B-04**
**12.0**
$C_1$ $^{1}A$

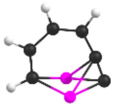

**B-05**
**12.8**
$C_s$ $^{1}A'$

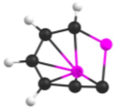

**B-06**
**13.1**
$C_1$ $^{1}A$

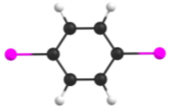

**B-07**
**13.9**
$D_{2h}$ $^{1}A_g$

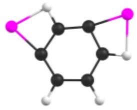

**B-08**
**14.1**
$C_s$ $^{1}A'$

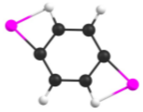

**B-09**
**14.5**
$C_{2h}$ $^{1}A_g$

**B-10**
**14.6**
$C_1$ $^{1}A$

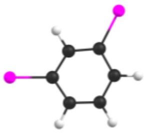

**B-11**
**14.7**
$C_{2v}$ $^{1}A_1$

**B-12**
**15.0**
$C_{2h}$ $^{1}A_g$

**B-13**
**15.3**
$C_{2v}$ $^{1}A_1$

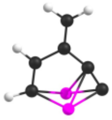

**B-14**
**16.1**
$C_s$ $^{1}A'$

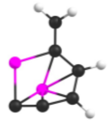

**B-15**
**16.8**
$C_1$ $^{1}A$

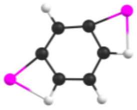

**B-16**
**17.2**
$C_{2v}$ $^{1}A_1$

**B-17**
**19.1**
$D_{2h}$ $^{1}A_g$

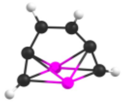

**B-18**
**20.8**
$C_1$ $^{1}A$

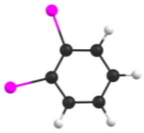

**B-19**
**21.2**
$C_{2v}$ $^{1}A_1$

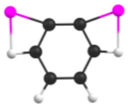

**B-20**
**21.4**
$C_{2v}$ $^{1}A_1$

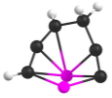

**B-21**
**21.8**
$C_1$ $^1\mathrm{A}$

**B-22**
**22.7**
$C_{2v}$ $^1\mathrm{A}_1$

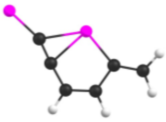

**B-23**
**24.4**
$C_s$ $^1\mathrm{A}'$

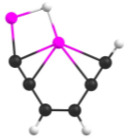

**B-24**
**25.5**
$C_s$ $^1\mathrm{A}'$

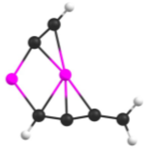

**B-25**
**25.9**
$C_s$ $^1\mathrm{A}'$

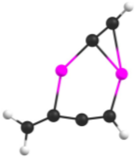

**B-26**
**26.2**
$C_s$ $^1\mathrm{A}'$

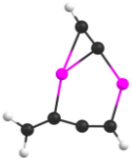

**B-27**
**26.4**
$C_s$ $^1\mathrm{A}'$

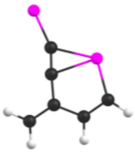

**B-28**
**27.1**
$C_s$ $^1\mathrm{A}'$

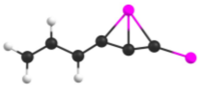

**B-29**
**27.5**
$C_s$ $^1\mathrm{A}'$

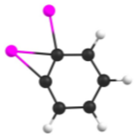

**B-30**
**27.6**
$C_1$ $^3\mathrm{A}$

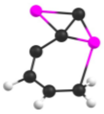

**B-31**
**27.6**
$C_1$ $^1\mathrm{A}$

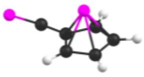

**B-32**
**27.9**
$C_s$ $^1\mathrm{A}'$

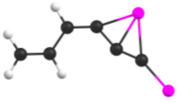

**B-33**
**28.3**
$C_s$ $^1\mathrm{A}'$

**B-34**
**29.4**
$C_s$ $^1\mathrm{A}'$

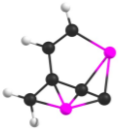

**B-35**
**29.5**
$C_1$ $^1\mathrm{A}$

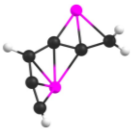

**B-36**
**29.7**
$C_1$ $^1\mathrm{A}$

**B-37**
**29.7**
$C_1$ $^1\mathrm{A}$

**B-38**
**29.8**
$C_s$ $^3\mathrm{A}''$

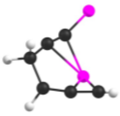

**B-39**
**31.1**
$C_1$ $^1\mathrm{A}$

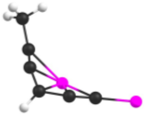

**B-40**
**31.2**
$C_1$ $^1\mathrm{A}$

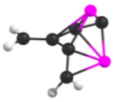

**B-41**
**31.9**
$C_1$ $^{1}$A

**B-42**
**32.1**
$C_1$ $^{1}$A

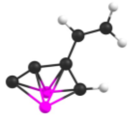

**B-43**
**32.4**
$C_1$ $^{1}$A

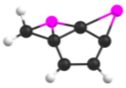

**B-44**
**32.9**
$C_1$ $^{1}$A

**B-45**
**33.1**
$C_1$ $^{1}$A

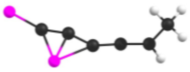

**B-46**
**33.1**
$C_1$ $^{1}$A

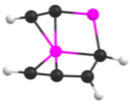

**B-47**
**33.1**
$C_1$ $^{1}$A

**B-48**
**33.1**
$C_1$ $^{1}$A

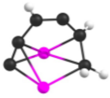

**B-49**
**33.3**
$C_1$ $^{1}$A

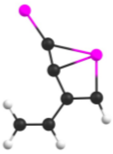

**B-50**
**33.4**
$C_s$ $^{1}$A′

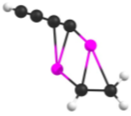

**B-51**
**33.4**
$C_1$ $^{1}$A

**B-52**
**33.4**
$C_1$ $^{1}$A

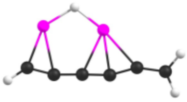

**B-53**
**33.5**
$C_s$ $^{1}$A′

**B-54**
**34.2**
$C_s$ $^{3}$A″

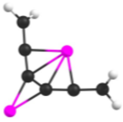

**B-55**
**34.3**
$C_2$ $^{1}$A

**B-56**
**34.9**
$C_1$ $^{1}$A

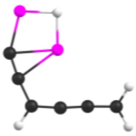

**B-57**
**35.4**
$C_s$ $^{1}$A′

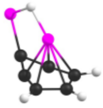

**B-58**
**36.0**
$C_s$ $^{1}$A′

**B-59**
**36.1**
$C_1$ $^{3}$A

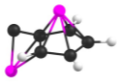

**B-60**
**36.4**
$C_1$ $^{3}$A

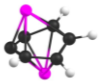

**B-61**
**36.6**

$C_1$ $^{1}\mathrm{A}$

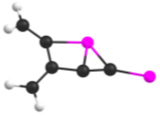

**B-62**
**36.7**

$C_1$ $^{1}\mathrm{A}$

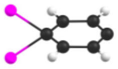

**B-63**
**36.8**

$C_{2v}$ $^{3}\mathrm{A}_1$

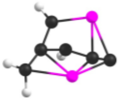

**B-64**
**37.6**

$C_1$ $^{1}\mathrm{A}$

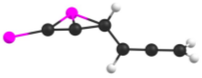

**B-65**
**37.8**

$C_1$ $^{1}\mathrm{A}$

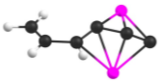

**B-66**
**38.7**

$C_1$ $^{1}\mathrm{A}$

**B-67**
**38.8**

$C_s$ $^{3}\mathrm{A}'$

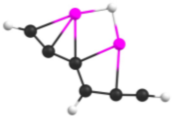

**B-68**
**39.8**

$C_s$ $^{1}\mathrm{A}'$

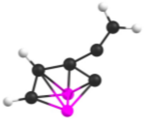

**B-69**
**40.0**

$C_s$ $^{1}\mathrm{A}'$

$C_6H_3Li_3$ stoichiometry

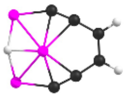

**C-01**
**0.0**
$C_s$ $^1A'$

**C-02**
**6.7**
$C_s$ $^1A'$

**C-03**
**14.9**
$C_1$ $^1A$

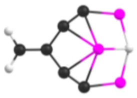

**C-04**
**15.2**
$C_s$ $^1A'$

**C-05**
**15.7**
$C_1$ $^1A$

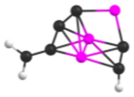

**C-06**
**16.2**
$C_s$ $^1A'$

**C-07**
**16.2**
$C_s$ $^1A'$

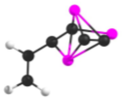

**C-08**
**17.8**
$C_1$ $^1A$

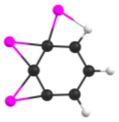

**C-09**
**18.6**
$C_s$ $^1A'$

**C-10**
**20.4**
$C_1$ $^1A$

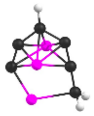

**C-11**
**20.5**
$C_s$ $^1A'$

**C-12**
**21.1**
$C_1$ $^1A$

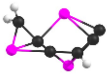

**C-13**
**21.2**
$C_1$ $^1A$

**C-14**
**21.8**
$C_1$ $^1A$

**C-15**
**22.0**
$C_1$ $^1A$

**C-16**
**22.5**
$C_1$ $^1A$

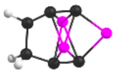

**C-17**
**22.6**
$C_1$ $^1A$

**C-18**
**22.7**
$C_s$ $^1A'$

**C-19**
**22.8**
$C_1$ $^1A$

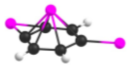

**C-20**
**23.0**
$C_1$ $^1A$

**C-21**
**23.1**
$C_1$ $^1\mathrm{A}$

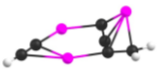

**C-22**
**23.1**
$C_1$ $^1\mathrm{A}$

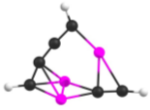

**C-23**
**23.2**
$C_s$ $^1\mathrm{A}'$

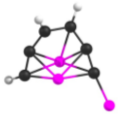

**C-24**
**23.5**
$C_1$ $^1\mathrm{A}$

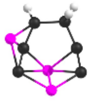

**C-25**
**24.1**
$C_1$ $^1\mathrm{A}$

**C-26**
**24.6**
$C_s$ $^1\mathrm{A}'$

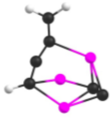

**C-27**
**25.2**
$C_1$ $^1\mathrm{A}$

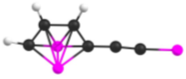

**C-28**
**26.1**
$C_s$ $^1\mathrm{A}'$

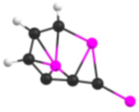

**C-29**
**26.1**
$C_1$ $^1\mathrm{A}$

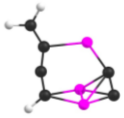

**C-30**
**26.2**
$C_s$ $^1\mathrm{A}'$

**C-31**
**26.7**
$C_1$ $^1\mathrm{A}$

**C-32**
**26.9**
$C_s$ $^1\mathrm{A}'$

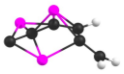

**C-33**
**27.4**
$C_1$ $^1\mathrm{A}$

**C-34**
**27.6**
$C_1$ $^1\mathrm{A}$

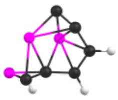

**C-35**
**29.6**
$C_1$ $^1\mathrm{A}$

**C-36**
**29.7**
$C_1$ $^1\mathrm{A}$

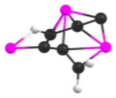

**C-37**
**30.0**
$C_1$ $^1\mathrm{A}$

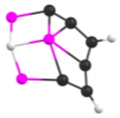

**C-38**
**30.1**
$C_1$ $^1\mathrm{A}$

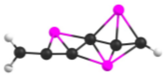

**C-39**
**30.2**
$C_1$ $^1\mathrm{A}$

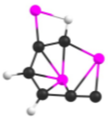

**C-40**
**31.9**
$C_1$ $^1\mathrm{A}$

**C-41**
**32.0**
$C_1$ $^1$A

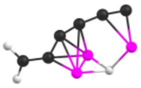

**C-42**
**32.1**
$C_s$ $^1$A′

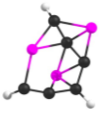

**C-43**
**32.8**
$C_1$ $^1$A

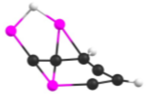

**C-44**
**32.9**
$C_1$ $^1$A

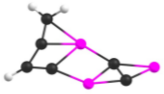

**C-45**
**33.3**
$C_1$ $^1$A

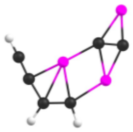

**C-46**
**33.6**
$C_1$ $^1$A

**C-47**
**33.8**
$C_1$ $^1$A

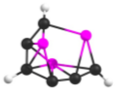

**C-48**
**33.9**
$C_1$ $^1$A

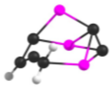

**C-49**
**33.9**
$C_1$ $^1$A

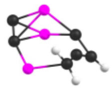

**C-50**
**34.0**
$C_1$ $^1$A

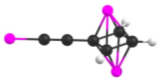

**C-51**
**34.3**
$C_{2v}$ $^1$A$_1$

**C-52**
**34.6**
$C_1$ $^1$A

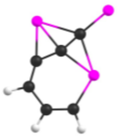

**C-53**
**34.6**
$C_s$ $^1$A′

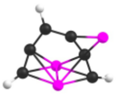

**C-54**
**34.9**
$C_1$ $^1$A

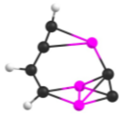

**C-55**
**35.1**
$C_s$ $^1$A′

**C-56**
**35.1**
$C_1$ $^1$A

**C-57**
**35.1**
$C_s$ $^1$A′

**C-58**
**35.2**
$C_1$ $^1$A

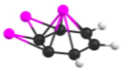

**C-59**
**35.4**
$C_1$ $^3$A

**C-60**
**35.4**
$C_1$ $^3$A

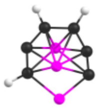

**C-61**
**35.9**
$C_s$ $^3A''$

**C-62**
**36.0**
$C_1$ $^1A$

**C-63**
**36.0**
$C_1$ $^1A$

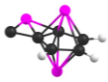

**C-64**
**36.3**
$C_s$ $^3A''$

**C-65**
**36.7**
$C_1$ $^1A$

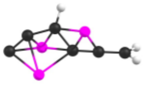

**C-66**
**36.8**
$C_1$ $^1A$

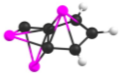

**C-67**
**36.8**
$C_1$ $^3A$

**C-68**
**36.9**
$C_1$ $^1A$

**C-69**
**37.0**
$C_s$ $^1A'$

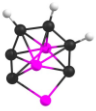

**C-70**
**37.5**
$C_s$ $^3A''$

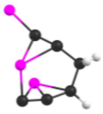

**C-71**
**37.8**
$C_1$ $^1A$

**C-72**
**38.0**
$C_1$ $^1A$

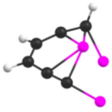

**C-73**
**38.1**
$C_1$ $^3A$

**C-74**
**38.4**
$C_1$ $^1A$

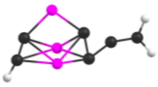

**C-75**
**38.7**
$C_s$ $^1A'$

**C-76**
**38.7**
$C_1$ $^1A$

**C-77**
**38.9**
$C_s$ $^1A'$

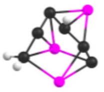

**C-78**
**38.9**
$C_1$ $^1A$

**C-79**
**39.4**
$C_1$ $^3A$

**C-80**
**40.0**
$C_1$ $^1A$

$C_6H_2Li_4$ stoichiometry

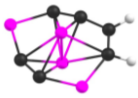
**D-01**
**0.0**
$C_s$ $^1A'$


**D-02**
**3.5**
$C_s$ $^1A'$


**D-03**
**3.6**
$C_1$ $^1A$


**D-04**
**6.4**
$C_{2h}$ $^1A_g$


**D-05**
**6.5**
$C_1$ $^1A$

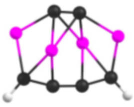
**D-06**
**8.6**
$C_2$ $^1A$

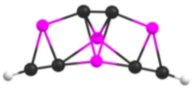
**D-07**
**9.0**
$C_{2v}$ $^1A_1$

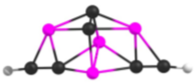
**D-08**
**9.0**
$C_{2v}$ $^1A_1$

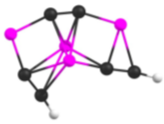
**D-09**
**9.3**
$C_s$ $^1A'$

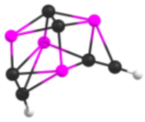
**D-10**
**9.3**
$C_1$ $^1A$

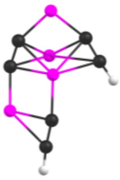
**D-11**
**9.9**
$C_1$ $^1A$

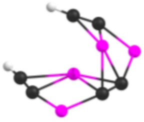
**D-12**
**10.1**
$C_1$ $^1A$


**D-13**
**10.4**
$C_1$ $^1A$

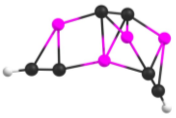
**D-14**
**10.5**
$C_1$ $^1A$

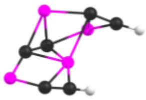
**D-15**
**10.5**
$C_1$ $^1A$

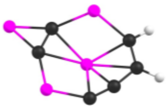
**D-16**
**13.8**
$C_1$ $^1A$

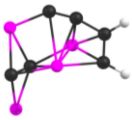
**D-17**
**15.3**
$C_1$ $^1A$

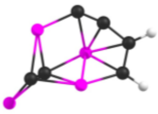
**D-18**
**15.7**
$C_1$ $^1A$


**D-19**
**16.3**
$C_1$ $^1A$

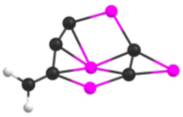
**D-20**
**16.8**
$C_1$ $^1A$

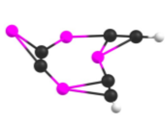

**D-21**
17.5
$C_1$ $^1$A

**D-22**
17.6
$C_1$ $^1$A

**D-23**
18.3
$C_1$ $^1$A

**D-24**
18.7
$C_s$ $^1$A′

**D-25**
18.8
$C_s$ $^1$A′

**D-26**
18.9
$C_1$ $^1$A

**D-27**
19.0
$C_1$ $^1$A

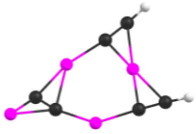

**D-28**
19.1
$C_1$ $^1$A

**D-29**
21.1
$C_1$ $^1$A

**D-30**
22.2
$C_2$ $^1$A

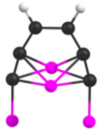

**D-31**
22.3
$C_1$ $^3$A

**D-32**
23.0
$C_2$ $^1$A

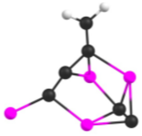

**D-33**
23.7
$C_1$ $^1$A

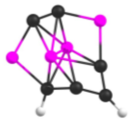

**D-34**
24.2
$C_s$ $^1$A′

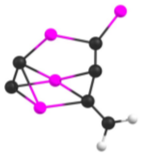

**D-35**
25.2
$C_1$ $^1$A

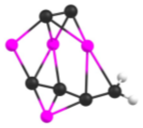

**D-36**
25.3
$C_1$ $^1$A

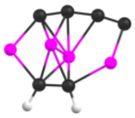

**D-37**
26.1
$C_1$ $^1$A

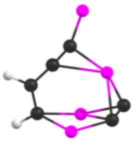

**D-38**
26.4
$C_1$ $^1$A

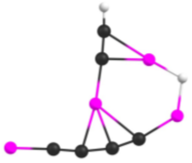

**D-39**
26.5
$C_s$ $^1$A′

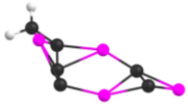

**D-40**
28.2
$C_1$ $^1$A

**D-41**
**29.4**
$C_1$ $^{1}\mathrm{A}$

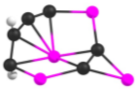

**D-42**
**30.1**
$C_1$ $^{1}\mathrm{A}$

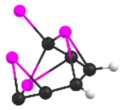

**D-43**
**30.6**
$C_1$ $^{1}\mathrm{A}$

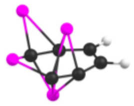

**D-44**
**30.8**
$C_1$ $^{3}\mathrm{A}$

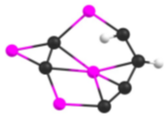

**D-45**
**31.4**
$C_1$ $^{1}\mathrm{A}$

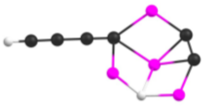

**D-46**
**32.2**
$C_1$ $^{1}\mathrm{A}$

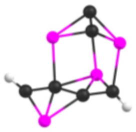

**D-47**
**33.4**
$C_1$ $^{1}\mathrm{A}$

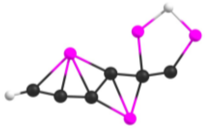

**D-48**
**33.9**
$C_1$ $^{1}\mathrm{A}$

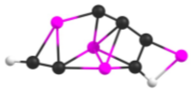

**D-49**
**35.0**
$C_1$ $^{1}\mathrm{A}$

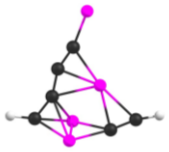

**D-50**
**35.1**
$C_s$ $^{1}\mathrm{A}'$

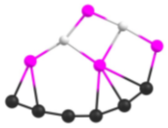

**D-51**
**35.6**
$C_s$ $^{1}\mathrm{A}'$

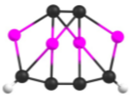

**D-52**
**35.7**
$C_2$ $^{3}\mathrm{B}$

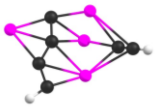

**D-53**
**35.8**
$C_1$ $^{1}\mathrm{A}$

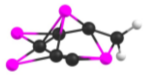

**D-54**
**36.1**
$C_1$ $^{1}\mathrm{A}$

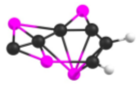

**D-55**
**36.2**
$C_1$ $^{1}\mathrm{A}$

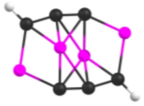

**D-56**
**36.4**
$C_1$ $^{3}\mathrm{A}$

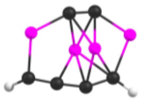

**D-57**
**36.8**
$C_1$ $^{3}\mathrm{A}$

**D-58**
**38.2**
$C_{2v}$ $^{3}\mathrm{B}_1$

**D-59**
**38.3**
$C_2$ $^{3}\mathrm{B}$

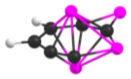

**D-60**
**38.5**
$C_s$ $^{3}\mathrm{A}''$

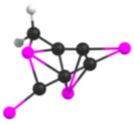

**D-61**
**38.6**

$C_1$ $^{1}\mathrm{A}$

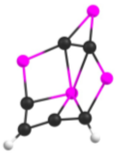

**D-62**
**38.7**

$C_1$ $^{1}\mathrm{A}$

**D-63**
**38.9**

$C_1$ $^{1}\mathrm{A}$

**D-64**
**39.3**

$C_s$ $^{1}\mathrm{A}'$

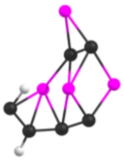

**D-65**
**39.4**

$C_1$ $^{1}\mathrm{A}$

**D-66**
**39.4**

$C_1$ $^{1}\mathrm{A}$

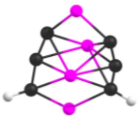

**D-67**
**39.6**

$C_1$ $^{3}\mathrm{A}$

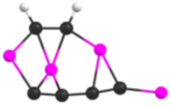

**D-68**
**39.8**

$C_1$ $^{1}\mathrm{A}$

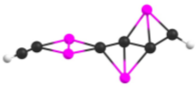

**D-69**
**39.9**

$C_1$ $^{1}\mathrm{A}$

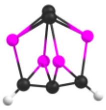

**D-70**
**40.8**

$C_2$ $^{3}\mathrm{B}$

*$C_6HLi_5$ stoichiometry*

**E-01**
**0.0**
$C_1$ $^1A$

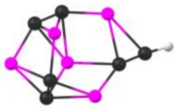

**E-02**
**3.8**
$C_1$ $^1A$

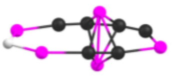

**E-03**
**4.3**
$C_s$ $^1A'$

**E-04**
**4.8**
$C_1$ $^1A$

**E-05**
**7.1**
$C_1$ $^1A$

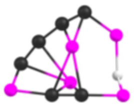

**E-06**
**8.8**
$C_1$ $^1A$

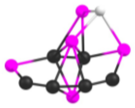

**E-07**
**8.9**
$C_1$ $^1A$

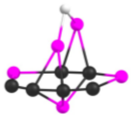

**E-08**
**9.1**
$C_1$ $^1A$

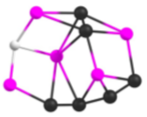

**E-09**
**9.4**
$C_1$ $^1A$

**E-10**
**9.5**
$C_1$ $^1A$

**E-11**
**10.0**
$C_1$ $^1A$

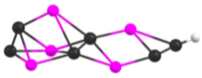

**E-12**
**15.3**
$C_1$ $^1A$

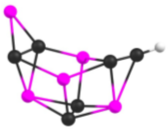

**E-13**
**16.1**
$C_1$ $^1A$

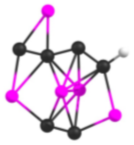

**E-14**
**17.9**
$C_s$ $^1A'$

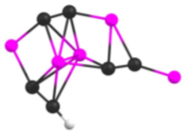

**E-15**
**18.0**
$C_s$ $^1A'$

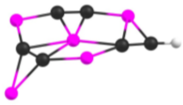

**E-16**
**19.0**
$C_1$ $^1A$

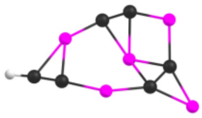

**E-17**
**19.7**
$C_1$ $^1A$

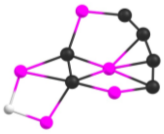

**E-18**
**20.4**
$C_1$ $^1A$

**E-19**
**20.8**
$C_1$ $^1A$

**E-20**
**21.3**
$C_1$ $^1A$

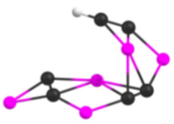

**E-21**
**21.3**
$C_1$ $^1\mathrm{A}$

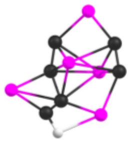

**E-22**
**22.0**
$C_1$ $^1\mathrm{A}$

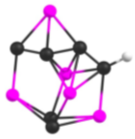

**E-23**
**23.3**
$C_1$ $^1\mathrm{A}$

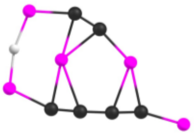

**E-24**
**24.6**
$C_s$ $^1\mathrm{A}'$

**E-25**
**25.1**
$C_1$ $^1\mathrm{A}$

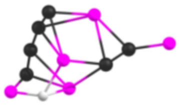

**E-26**
**25.8**
$C_1$ $^1\mathrm{A}$

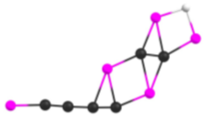

**E-27**
**26.8**
$C_s$ $^1\mathrm{A}'$

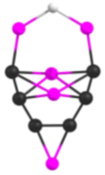

**E-28**
**27.5**
$C_{2v}$ $^1\mathrm{A}_1$

**E-29**
**27.6**
$C_1$ $^1\mathrm{A}$

**E-30**
**28.0**
$C_s$ $^1\mathrm{A}'$

**E-31**
**29.2**
$C_1$ $^1\mathrm{A}$

**E-32**
**29.8**
$C_1$ $^1\mathrm{A}$

**E-33**
**30.1**
$C_1$ $^1\mathrm{A}$

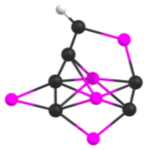

**E-34**
**30.1**
$C_s$ $^1\mathrm{A}'$

**E-35**
**30.6**
$C_1$ $^1\mathrm{A}$

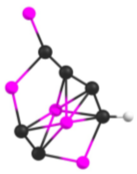

**E-36**
**30.9**

$C_s$ $^1A'$

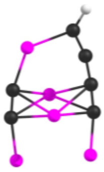

**E-37**
**35.9**

$C_s$ $^3A'$

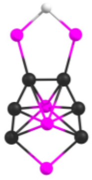

**E-38**
**36.0**

$C_{2v}$ $^1A_1$

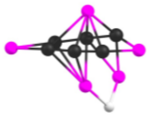

**E-39**
**36.6**

$C_1$ $^1A$

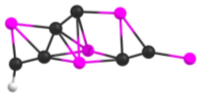

**E-40**
**39.0**

$C_s$ $^1A'$

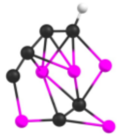

**E-41**
**40.6**

$C_1$ $^3A$

**E-42**
**41.0**

$C_1$ $^3A$

*$C_6Li_6$ stoichiometry*

**F-01**
**0.0**
$C_1$ $^1A$

**F-02**
**8.5**
$D_3$ $^1A_1$

**F-03**
**10.7**
$C_s$ $^1A'$

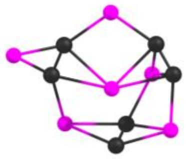

**F-04**
**12.4**
$C_1$ $^1A$

**F-05**
**12.7**
$C_1$ $^1A$

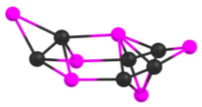

**F-06**
**13.4**
$C_s$ $^1A'$

**F-07**
**15.8**
$C_{2v}$ $^1A_1$

**F-08**
**19.2**
$C_1$ $^1A$

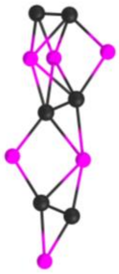

**F-09**
**33.0**
$C_s$ $^1A'$

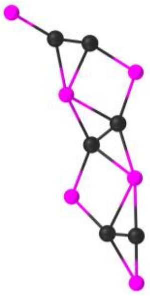

**F-10**
**37.5**
$C_1$ $^1A$

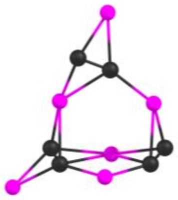

**F-11**
**37.5**
$C_1$ $^1A$

**F-12**
**46.1**
$C_1$ $^3A$

*$C_6Na_6$ stoichiometry*

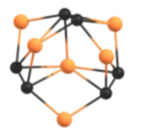

**G-01**

**0.0**

$C_1$ ${}^1\mathrm{A}$

**G-02**

**4.7**

$D_3$ ${}^1\mathrm{A}_1$

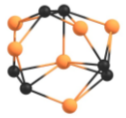

**G-03**

**5.0**

$C_1$ ${}^1\mathrm{A}$

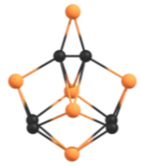

**G-04**

**5.2**

$C_{2v}$ ${}^1\mathrm{A}_1$

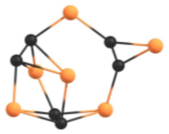

**G-05**

**6.2**

$C_1$ ${}^1\mathrm{A}$

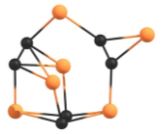

**G-06**

**6.8**

$C_s$ ${}^1\mathrm{A}'$

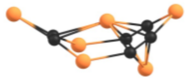

**G-07**

**6.9**

$C_s$ ${}^1\mathrm{A}'$

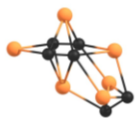

**G-08**

**7.2**

$C_s$ ${}^1\mathrm{A}'$

**G-09**

**7.2**

$C_1$ ${}^1\mathrm{A}$

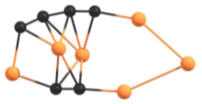

**G-10**

**7.3**

$C_1$ ${}^1\mathrm{A}$

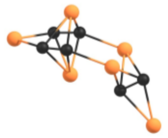

**G-11**

**7.8**

$C_s$ ${}^1\mathrm{A}'$

**G-12**

**8.5**

$C_1$ ${}^1\mathrm{A}$

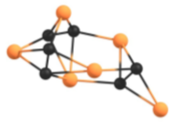

**G-13**

**8.6**

$C_1$ ${}^1\mathrm{A}$

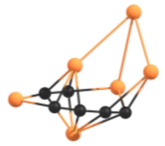

**G-14**

**9.9**

$C_1$ ${}^1\mathrm{A}$

**G-15**

**10.0**

$C_s$ ${}^1\mathrm{A}'$

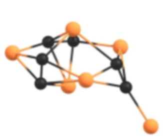

**G-16**
**11.6**
$C_1$ $^1A$

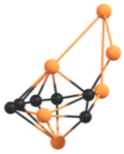

**G-17**
**12.0**
$C_1$ $^1A$

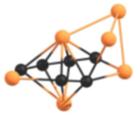

**G-18**
**12.5**
$C_1$ $^1A$

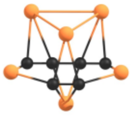

**G-19**
**12.8**
$C_s$ $^1A'$

**G-20**
**12.8**
$C_1$ $^1A$

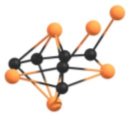

**G-21**
**13.3**
$C_1$ $^1A$

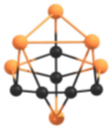

**G-22**
**13.5**
$C_s$ $^1A'$

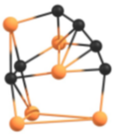

**G-23**
**14.1**
$C_1$ $^1A$

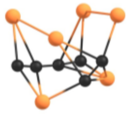

**G-24**
**14.4**
$C_1$ $^1A$

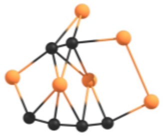

**G-25**
**14.9**
$C_1$ $^1A$

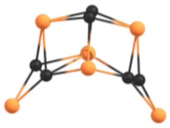

**G-26**
**16.1**
$C_2$ $^1A$

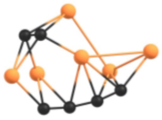

**G-27**
**16.6**
$C_1$ $^1A$

**G-28**
**17.3**
$C_s$ $^1A'$

**G-29**
**17.4**
$C_1$ $^1A$

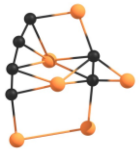

**G-30**
**17.4**
$C_1$ $^1A$

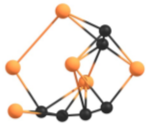

**G-31**
**17.5**
$C_1$ $^1A$

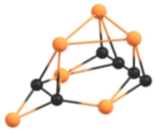

**G-32**
**17.6**
$C_1$ $^1A$

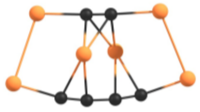

**G-33**
**17.7**
$C_1$ $^3A$

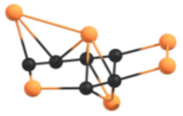

**G-34**
**17.9**
$C_1$ $^3A$

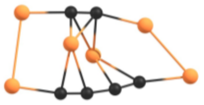

**G-35**
**17.9**
$C_1$ $^3A$

**G-36**
**18.0**
$C_1$ $^{1}$A

**G-37**
**18.0**
$C_1$ $^{1}$A

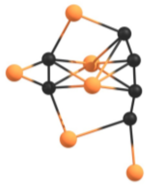

**G-38**
**18.2**
$C_1$ $^{3}$A

**G-39**
**18.2**
$C_1$ $^{3}$A

**G-40**
**18.2**
$C_1$ $^{3}$A

**G-41**
**19.3**
$C_1$ $^{3}$A

**G-42**
**19.5**
$C_1$ $^{3}$A

**G-43**
**19.7**
$C_1$ $^{1}$A

**G-44**
**20.0**
$C_s$ $^{1}$A′

*$C_6K_6$ stoichiometry*

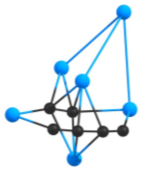

**H-01**
0.0
$C_1$ $^1\mathrm{A}$

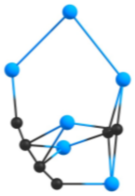

**H-02**
1.7
$C_1$ $^1\mathrm{A}$

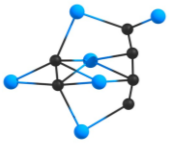

**H-03**
3.1
$C_1$ $^3\mathrm{A}$

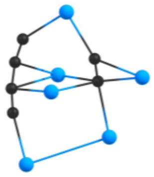

**H-04**
3.2
$C_1$ $^1\mathrm{A}$

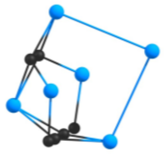

**H-05**
3.8
$C_s$ $^1\mathrm{A}'$

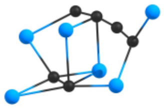

**H-06**
3.8
$C_1$ $^3\mathrm{A}$

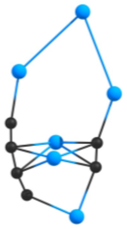

**H-07**
4.2
$C_1$ $^1\mathrm{A}$

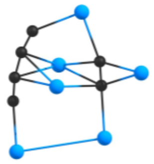

**H-08**
4.3
$C_1$ $^3\mathrm{A}$

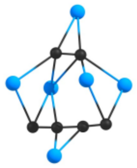

**H-09**
4.3
$C_1$ $^3\mathrm{A}$

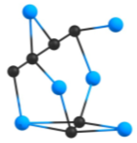

**H-10**
4.4
$C_s$ $^1\mathrm{A}'$

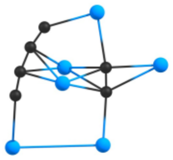

**H-11**
4.7
$C_1$ $^3\mathrm{A}$

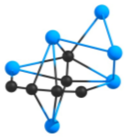

**H-12**
4.9
$C_1$ $^1\mathrm{A}$

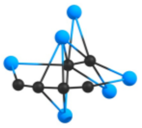

**H-13**
4.9
$C_1$ $^3\mathrm{A}$

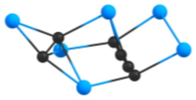

**H-14**
5.0
$C_s$ $^1\mathrm{A}'$

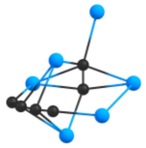

**H-15**
5.0
$C_1$ $^3\mathrm{A}$

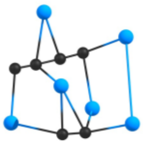

**H-16**
**5.0**
$C_1$ $^{1}\mathrm{A}$

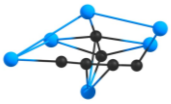

**H-17**
**5.2**
$C_1$ $^{3}\mathrm{A}$

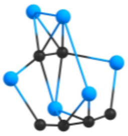

**H-18**
**5.2**
$C_s$ $^{1}\mathrm{A}'$

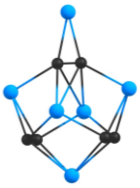

**H-19**
**5.5**
$C_{2v}$ $^{1}\mathrm{A}_1$

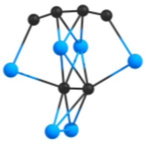

**H-20**
**5.5**
$C_s$ $^{1}\mathrm{A}'$

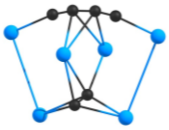

**H-21**
**5.7**
$C_1$ $^{3}\mathrm{A}$

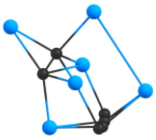

**H-22**
**5.7**
$C_s$ $^{1}\mathrm{A}'$

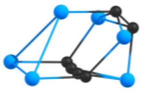

**H-23**
**6.0**
$C_s$ $^{1}\mathrm{A}'$

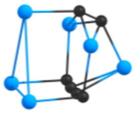

**H-24**
**6.1**
$C_s$ $^{1}\mathrm{A}'$

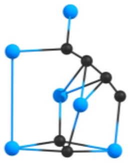

**H-25**
**6.4**
$C_1$ $^{3}\mathrm{A}$

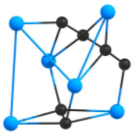

**H-26**
**6.5**
$C_1$ $^{3}\mathrm{A}$

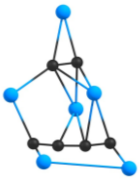

**H-27**
**6.7**
$C_1$ $^{1}\mathrm{A}$

**H-28**
**7.2**
$C_1$ $^{3}\mathrm{A}$

**H-29**
**7.4**
$C_1$ $^{3}\mathrm{A}$

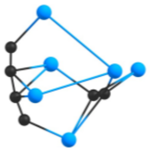

**H-30**
**7.7**
$C_1$ $^{1}\mathrm{A}$

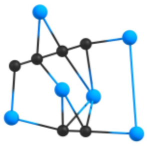

**H-31**
**7.8**
$C_1$ $^3A$

**H-32**
**7.9**
$C_1$ $^3A$

**H-33**
**8.0**
$C_1$ $^3A$

**H-34**
**8.5**
$C_1$ $^3A$

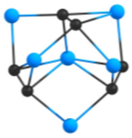

**H-35**
**9.3**
$C_1$ $^1A$

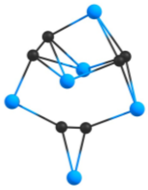

**H-36**
**9.3**
$C_s$ $^1A'$

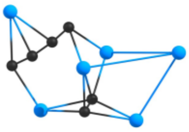

**H-37**
**9.5**
$C_1$ $^1A$

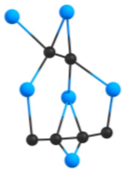

**H-38**
**9.9**
$C_1$ $^3A$

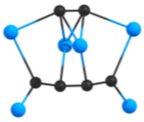

**H-39**
**10.0**
$C_1$ $^3A$

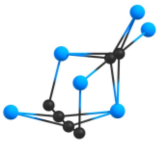

**H-40**
**10.0**
$C_1$ $^3A$

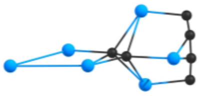

**H-41**
**10.6**
$C_s$ $^1A'$

**H-42**
**10.6**
$C_s$ $^1A'$

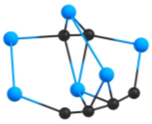

**H-43**
**10.6**
$C_1$ $^3A$

**H-44**
**10.7**
$C_1$ $^1A$

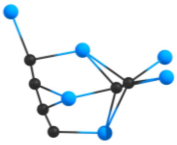

**H-45**
**11.0**
$C_1$ $^3A$

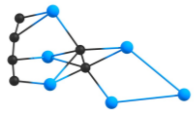

**H-46**
**11.5**
$C_1$ $^1$A

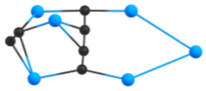

**H-47**
**11.6**
$C_s$ $^1$A′

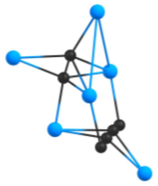

**H-48**
**12.0**
$C_s$ $^3$A′

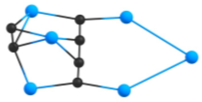

**H-49**
**12.2**
$C_1$ $^1$A

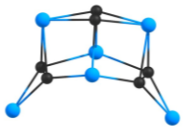

**H-50**
**12.3**
$C_1$ $^1$A

**H-51**
**13.2**
$C_s$ $^1$A′

**H-52**
**13.2**
$C_2$ $^1$A

**H-53**
**13.3**
$C_s$ $^1$A′

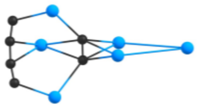

**H-54**
**13.5**
$C_s$ $^1$A′

**H-55**
**13.6**
$C_s$ $^1$A′

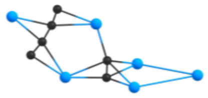

**H-56**
**15.3**
$C_s$ $^1$A′

**H-57**
**18.8**
$C_2$ $^1$A

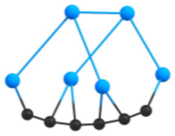

**H-58**
**19.7**
$C_s$ $^1$A′

*$C_6Rb_6$ stoichiometry*

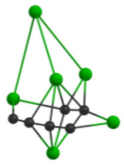

**I-01**
**0.0**
$C_1$ $^1\mathrm{A}$

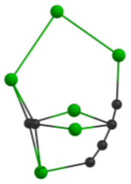

**I-02**
**0.9**
$C_1$ $^1\mathrm{A}$

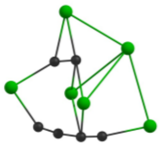

**I-03**
**1.7**
$C_s$ $^1\mathrm{A}'$

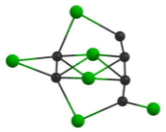

**I-04**
**1.9**
$C_1$ $^1\mathrm{A}$

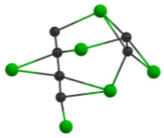

**I-05**
**2.1**
$C_1$ $^1\mathrm{A}$

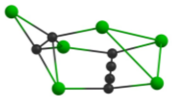

**I-06**
**2.4**
$C_s$ $^1\mathrm{A}'$

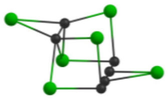

**I-07**
**2.5**
$C_1$ $^3\mathrm{A}$

**I-08**
**2.5**
$C_s$ $^1\mathrm{A}'$

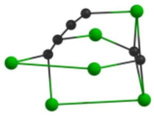

**I-09**
**2.6**
$C_1$ $^1\mathrm{A}$

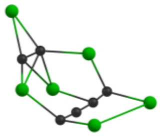

**I-10**
**2.7**
$C_1$ $^1\mathrm{A}$

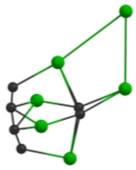

**I-11**
**2.7**
$C_s$ $^1\mathrm{A}'$

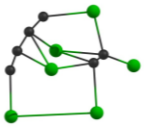

**I-12**
**2.9**
$C_1$ $^1\mathrm{A}$

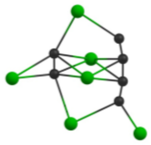

**I-13**
**3.0**
$C_1$ $^1\mathrm{A}$

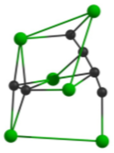

**I-14**
**3.6**
$C_1$ $^3\mathrm{A}$

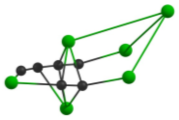

**I-15**
**3.9**
$C_1$ $^1\mathrm{A}$

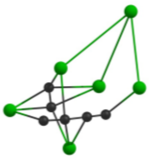

**I-16**

**4.3**

$C_1$ $^{1}\mathrm{A}$

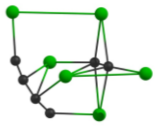

**I-17**

**4.5**

$C_1$ $^{3}\mathrm{A}$

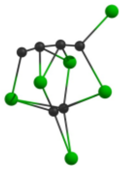

**I-18**

**5.0**

$C_1$ $^{3}\mathrm{A}$

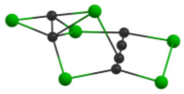

**I-19**

**5.4**

$C_1$ $^{3}\mathrm{A}$

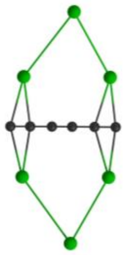

**I-20**

**11.0**

$C_{2v}$ $^{1}\mathrm{A}_1$

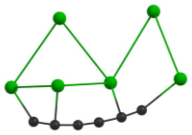

**I-21**

**11.6**

$C_1$ $^{1}\mathrm{A}$

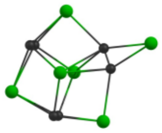

**I-22**

**12.4**

$C_{2v}$ $^{1}\mathrm{A}_1$

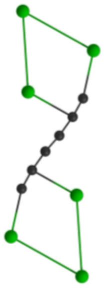

**I-23**

**12.7**

$C_{2h}$ $^{1}\mathrm{A}_g$

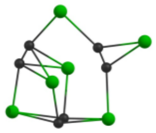

**I-24**

**16.1**

$C_1$ $^{1}\mathrm{A}$

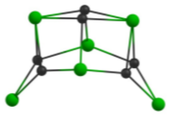

**I-25**

**17.3**

$C_1$ $^{1}\mathrm{A}$

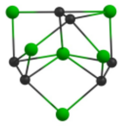

**I-26**

**18.7**

$C_1$ $^{1}\mathrm{A}$

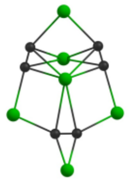

**I-27**

**20.6**

$C_s$ $^{1}\mathrm{A}'$

*$C_6Cs_6$ stoichiometry*

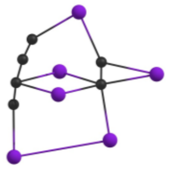

**J-01**
**0.0**

$C_s$ $^1A'$

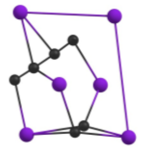

**J-02**
**0.6**

$C_1$ $^1A$

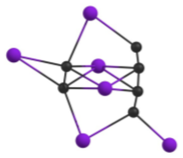

**J-03**
**0.7**

$C_1$ $^3A$

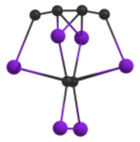

**J-04**
**0.9**

$C_{2v}$ $^1A_1$

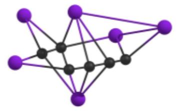

**J-05**
**1.0**

$C_1$ $^1A$

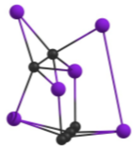

**J-06**
**1.2**

$C_1$ $^1A$

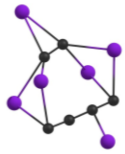

**J-07**
**1.4**

$C_1$ $^3A$

**J-08**
**1.7**

$C_1$ $^1A$

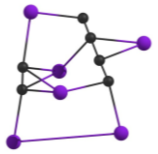

**J-09**
**2.2**

$C_1$ $^1A$

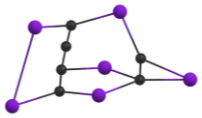

**J-10**
**2.4**

$C_1$ $^1A$

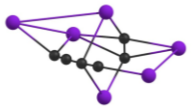

**J-11**
**2.5**

$C_1$ $^3A$

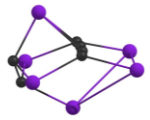

**J-12**
**3.2**

$C_s$ $^1A'$

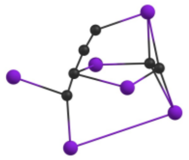

**J-13**
**3.7**

$C_1$ $^3A$

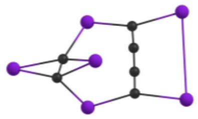

**J-14**
**4.0**

$C_1$ $^3A$

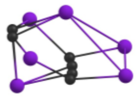

**J-15**
**4.0**

$C_s$ $^1A'$

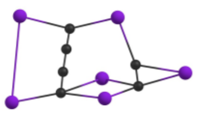

**J-16**
**4.1**
$C_1$ $^3A$

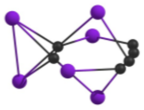

**J-17**
**4.5**
$C_1$ $^3A$

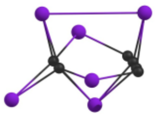

**J-18**
**5.8**
$C_1$ $^3A$

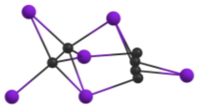

**J-19**
**6.3**
$C_1$ $^3A$

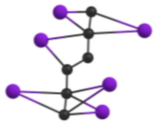

**J-20**
**6.3**
$C_1$ $^3A$

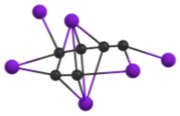

**J-21**
**7.4**
$C_1$ $^3A$

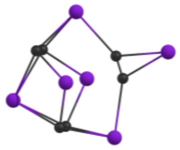

**J-22**
**8.5**
$C_{2v}$ $^1A_1$

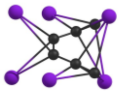

**J-23**
**8.9**
$C_1$ $^3A$

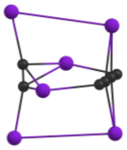

**J-24**
**9.7**
$C_1$ $^3A$

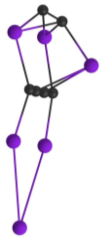

**J-25**
**10.3**
$C_s$ $^1A'$

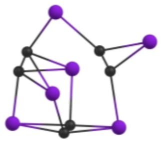

**J-26**
**11.4**
$C_s$ $^1A'$

**J-27**
**12.0**
$C_1$ $^3A$

**J-28**
**12.7**
$C_s$ $^1A'$

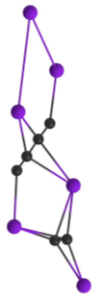

**J-29**
**13.5**
$C_1$ $^1A$

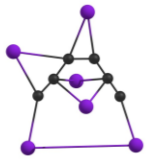

**J-30**
**14.3**
$C_1$ $^3A$

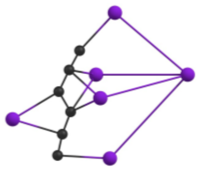

**J-31**
**14.8**

$C_s$ $^{1}A'$

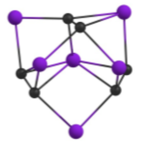

**J-32**
**16.3**

$C_1$ $^{1}A$

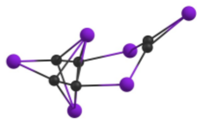

**J-33**
**17.1**

$C_s$ $^{1}A'$

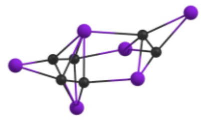

**J-34**
**17.8**

$C_s$ $^{1}A'$

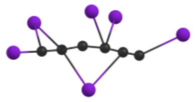

**J-35**
**18.4**

$C_1$ $^{3}A$

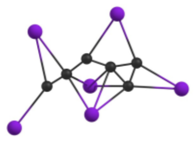

**J-36**
**19.0**

$C_1$ $^{3}A$

# REFERENCES

1 P. von Ragué Schleyer, Remarkable structures of lithium compounds, *Pure Appl. Chem.*, 1984, **56**, 151–162.

2 Y. Apeloig, Geometries and Energies of Dilithioethylene Isomers and of Vinyl Lithium, an Ab Initio Study, *Isr. J. Chem.*, 1980, **20**, 43–50.

3 E. D. Jemmis, J. Chandrasekhar and P. von Ragué Schleyer, The Unusual Structures, Energies, and Bonding of Lithium-Substituted Alienes, Propynes, and Cyclopropenes, *J. Am. Chem. Soc.*, 1979, **101**, 2848–2856.

4 W. Priester, R. West and T. L. Chwang, Polylithium Compounds. 8. Synthesis of Allenes and Acetylenes from Perlithiopropyne, Trilithiobutyne, and Dilithio-3-methylbutyne, *J. Am. Chem. Soc.*, 1976, **98**, 8413–8421.

5 E. D. Jemmis and G. Gopakumar, in *The Chemistry of Organolithium Compounds Part 1*, 2004, pp. 1–45.

6 F. M. Bickelhaupt, N. J. R. V. E. Hommes, F. Guerra and E. J. Baerends, The Carbon - Lithium Electron Pair Bond in ( CH 3 Li ) n ( n ) 1 , 2 , 4 ), 1996, **7333**, 2923–2931.

7 F. M. Bickelhaupt, M. Solà and C. F. Guerra, Covalency in highly polar bonds. Structure and bonding of methylalkalimetal oligomers (CH3M)n (M = Li-Rb; n = 1, 4), *J. Chem. Theory Comput.*, 2006, **2**, 965–980.

8 O. Kwon, F. Sevin and M. L. McKee, Density functional calculations of methyllithium, t-butyllithium, and phenyllithium oligomers: Effect of hyperconjugation on conformation, *J. Phys. Chem. A*, 2001, **105**, 913–922.

9 R. A. Marcus, Skiing the reaction rate slopes, *Science (80-. ).*, 1992, **256**, 1523–1524.

10 E. G. Lewars, *Computational Chemistry: Introduction to the Theory and Applications of Molecular and Quantum Mechanics*, Springer, Netherlands, 2011.

11 J. L. Cabellos, F. Ortíz-Chi, A. Ramírez and G. Merino, 2013.

12 D. E. Goldberg, *Genetic Algorithms in Search, Optimization, and Machine Learning*, Addison-Wesley Reading, USA, 1989.

13 M. J. Frisch, G. W. Trucks, H. B. Schlegel, G. E. Scuseria, M. a. Robb, J. R. Cheeseman, G. Scalmani, V. Barone, G. a. Petersson, H. Nakatsuji, X. Li, M. Caricato, a. V. Marenich, J. Bloino, B. G. Janesko, R. Gomperts, B. Mennucci, H. P. Hratchian, J. V. Ortiz, a. F. Izmaylov, J. L. Sonnenberg, Williams, F. Ding, F. Lipparini, F. Egidi, J. Goings, B. Peng, A. Petrone, T. Henderson, D. Ranasinghe, V. G. Zakrzewski,

J. Gao, N. Rega, G. Zheng, W. Liang, M. Hada, M. Ehara, K. Toyota, R. Fukuda, J. Hasegawa, M. Ishida, T. Nakajima, Y. Honda, O. Kitao, H. Nakai, T. Vreven, K. Throssell, J. a. Montgomery Jr., J. E. Peralta, F. Ogliaro, M. J. Bearpark, J. J. Heyd, E. N. Brothers, K. N. Kudin, V. N. Staroverov, T. a. Keith, R. Kobayashi, J. Normand, K. Raghavachari, a. P. Rendell, J. C. Burant, S. S. Iyengar, J. Tomasi, M. Cossi, J. M. Millam, M. Klene, C. Adamo, R. Cammi, J. W. Ochterski, R. L. Martin, K. Morokuma, O. Farkas, J. B. Foresman and D. J. Fox, 2016, Gaussian 16, Revision C.01, Gaussian, Inc., Wallin.

14 S. K. Gregurick, M. H. Alexander and B. Hartke, Global geometry optimization of (Ar)n and B(Ar)n clusters using a modified genetic algorithm, *J. Chem. Phys.*, 1996, **104**, 2684–2691.

15 C. Adamo and V. Barone, Toward reliable density functional methods without adjustable parameters: The PBE0 model, *J. Chem. Phys.*, 1999, **110**, 6158–6170.

16 F. Weigend and R. Ahlrichs, Balanced basis sets of split valence, triple zeta valence and quadruple zeta valence quality for H to Rn: Design and assessment of accuracyElectronic supplementary information (ESI) available:[DETAILS]. See http://dx. doi. org/10.1039/b508541a, *Phys. Chem. Chem. Phys.*, 2005, **7**, 3297–3305.

17 J. P. Perdew, K. Burke and M. Ernzerhof, Generalized gradient approximation made simple, *Phys. Rev. Lett.*, 1996, **77**, 3865–3868.

18 M. Bursch, E. Caldeweyher, A. Hansen, H. Neugebauer, S. Ehlert and S. Grimme, Understanding and Quantifying London Dispersion Effects in Organometallic Complexes, *Acc. Chem. Res.*, 2019, **52**, 258–266.

19 J. D. Watts, J. Gauss and R. J. Bartlett, Coupled-cluster methods with noniterative triple excitations for restricted open-shell Hartree-Fock and other general single determinant reference functions. Energies and analytical gradients, *J. Chem. Phys.*, 1993, **98**, 8718–8733.

20 F. Weinhold and C. R. Landis, Natural Bond Orbitals and Extensions of Localized Bonding Concepts, *Chem. Educ. Res. Pr.*, 2001, **2**, 91–104.

21 D. Y. Zubarev and A. I. Boldyrev, Developing paradigms of chemical bonding: Adaptive natural density partitioning, *Phys. Chem. Chem. Phys.*, 2008, **10**, 5207–5217.

22 R. E. Dinnebier, U. Behrens and F. Olbrich, Lewis base-free phenyllithium: Determination of the solid-state structure by synchrotron powder diffraction, *J. Am. Chem. Soc.*, 1998, **120**, 1430–1433.

23 K. P. C. Vollhardt and N. E. Schore, *Organic Chemistry*, Macmillan International Higher Education, USA, 2007.

24 A. Streitwieser, Carbanion Ion Pairs and Triplets, *Acc. Chem. Res.*, 1984, **17**, 353–357.

25 G. Wittig and F. Bickelhaupt, o-Dilithium-benzol, *Angew. Chemie*, 1957, **69**, 93.

26 G. Wittig and F. Bickelhaupt, o-Dilithium-benzol, *Chem. Ber.*, 1958, **91**, 883–894.

27 H. J. S. Winkler and G. Wittig, Preparation and reactions of o-dilithiobenzene, *J. Org. Chem.*, 1963, **28**, 1733–1740.

28 M. Fossatelli, R. Den Besten, H. D. Verkruijsse and L. Brandsma, 1,3-Dilithiobenzene and 1,4-Dilithiobenzene, 1994, **528**, 527–528.

29 K. R. Flower, A. T. McGown, P. J. Miles, R. G. Pritchard and J. E. Warren, Isolation of 1,4-Li2-C6H4 and its reaction with [(Ph3P)AuCl], *Dalt. Trans.*, 2010, **39**, 3509–3520.

30 S. M. Bachrach and J. V. Miller, Structures and relative energies of polylithiated benzenes, *J. Org. Chem.*, 2002, **67**, 7389–7398.

31 S. M. Bachrach and A. C. Chamberlin, Deprotonation of Lithiated Benzenes, *J. Org. Chem.*, 2004, **69**, 2111–2122.

32 H. F. Bettinger and M. Filthaus, Halogen - Metal Exchange in 1 , 2-Dibromobenzene and the Possible Intermediacy of, *J. Org. Chem.*, 2007, 9750–9752.

33 K. K. Irikura, Experimental vibrational zero-point energies: Diatomic molecules, *J. Phys. Chem. Ref. data*, 2007, **36**, 389–397.

34 G. M. Plummer, E. Herbst and F. C. De Lucia, Submillimeter spectra and molecular constants of 6LiH, 7LiH, 6LiD, and 7LiD, *J. Chem. Phys.*, 1984, **81**, 4893–4897.

35 M. Schlosser, L. Guio and F. Leroux, Multiple hydrogen/lithium interconversions at the same benzene nucleus: Two at the most [3], *J. Am. Chem. Soc.*, 2001, **123**, 3822–3823.

36 D. Moreno, G. Martínez-Guajardo, A. Díaz-Celaya, J. M. Mercero, R. Dea Coss, N. Perez-Peralta and G. Merino, Re-examination of the C6Li6 structure: To be, or not to be symmetric, *Chem. - A Eur. J.*, 2013, **19**, 12668–12672.

37 J. R. Baran and R. J. Lagow, A New General Synthesis for Polylithium Organic Compounds, *J. Am. Chem. Soc.*, 1990, **112**, 9415–9416.

38 Y. Xie and H. F. Schaefer, Hexalithiobenzene: a D6h equilibrium geometry with six lithium atoms in bridging positions, *Chem. Phys. Lett.*, 1991, **179**, 563–567.

39 B. J. Smith, Hexalithiobenzene: beauty is in the eye of the beholder, *Chem. Phys. Lett.*, 1993, **207**, 403–406.

40 H. J. R. de Boer, O. S. Akkerman and F. Bickelhaupt, Carbanions as Intermediates in the Synthesis of Grignard Reagents, *Angew. Chemie Int. Ed. English*, 1988, **27**, 687–689.

41 R. N. Young, R. P. Quirk and L. J. Fetters, in *Anionic Polymerization*, Springer, 1984, pp. 1–90.

42 M. Morton, *Anionic polymerization: principles and practice*, Elsevier, 2012.

43 S. Carlotti, P. Desbois, C. Billouard and A. Deffieux, Reactivity control in anionic polymerization of ethylenic and heterocyclic monomers through formation of ‘ate’complexes, *Polym. Int.*, 2006, **55**, 1126–1131.

44 L. M. Jackman and J. Bortiatynski, AdV. Carbanion Chem. 1992, 1, 45.(b) Zune, C.; Jerome, R, *Prog Polym. Sci*, 1999, **24**, 631.

45 A. F. Halasa, D. N. Schulz, D. P. Tate and V. D. Mochel, in *Advances in organometallic chemistry*, Elsevier, 1980, vol. 18, pp. 55–97.

46 J. Smid, M. Van Beylen and T. E. Hogen-Esch, Perspectives on the contributions of Michael Szwarc to living polymerization, *Prog. Polym. Sci.*, 2006, **31**, 1041–1067.

47 D. Seyferth, Alkyl and aryl derivatives of the alkali metals: Strong bases and reactive nucleophiles. 2. Wilhelm schlenk’s organoalkali-metal chemistry. The metal displacement and the transmetalation reactions. Metalation of weakly acidic hydrocarbons. Superbases, *Organometallics*, 2009, **28**, 2–33.

48 M. Schlosser, Organoalkali Chemistry, *Organometallics Synth.*, 2013, 1–222.

49 D. B. Grotjahn, T. C. Pesch, M. A. Brewster and L. M. Ziurys, Synthesis of CH3K in the gas phase: Structural and mechanistic trends for monomeric, unsolvated CH3M and HCCM (M = Li, Na, K), *J. Am. Chem. Soc.*, 2000, **122**, 4735–4741.

50 E. Weiss and G. Sauermann, Preparation and Structure of Methylpotassium, *Angew. Chemie Int. Ed. English*, 1968, **7**, 133–134.

51 E. Weiss and G. Hencken, Über metall-alkyl-verbindungen. XII. verfeiner ung der kristallstruktur des methyllithiums, *J. Organomet. Chem.*, 1970, **21**, 265–268.

52 E. Weiss and H. Köster, Über Metallalkyl-und-aryl-Verbindungen, XIX. Darstellung und Kristallstruktur von Methylrubidium und Methylcaesium, *Chem. Ber.*, 1977, **110**, 717–720.

53 D. Seyferth, Alkyl and aryl derivatives of the alkali metals: Useful synthetic reagents as strong bases and potent nucleophiles. 1. Conversion of organic halides to organoalkali-metal compounds,

*Organometallics*, 2006, **25**, 2–24.

54 C. Tang, F. Gao, Z. Zhang, J. Kang, J. Zou, Y. Xu and W. Zhu, The properties of hydrogenated derivatives of the alkali atom coated clusters C6M6 (M = Li, Na): A density functional study, *Comput. Theor. Chem.*, 2015, **1071**, 46–52.

55 T. Lu and F. Chen, Multiwfn: a multifunctional wavefunction analyzer, *J. Comput. Chem.*, 2012, **33**, 580–592.